Article

Developmental Cell

Antagonistic systemin receptors integrate the activation and attenuation of systemic wound signaling in tomato

Graphical abstract

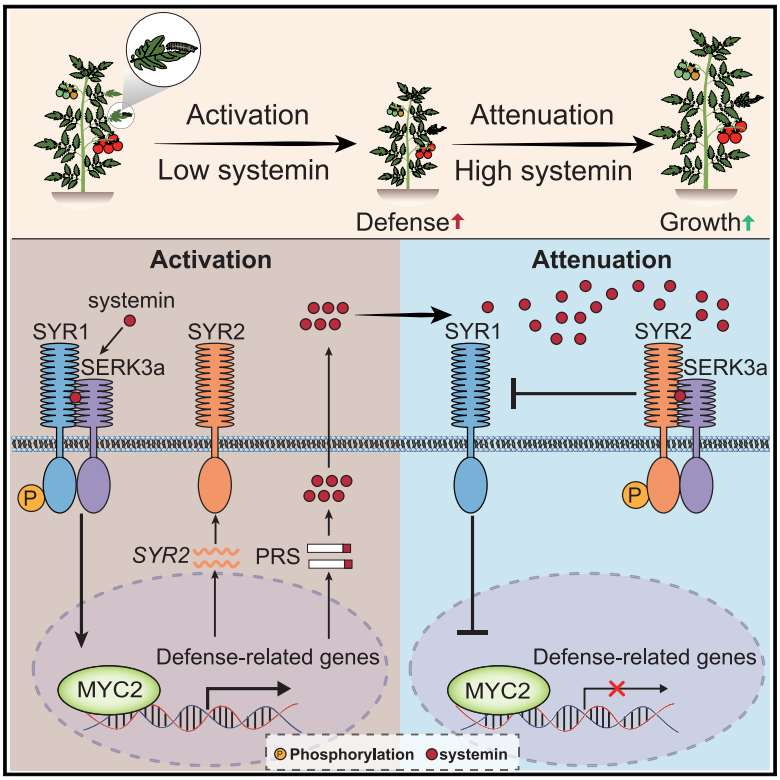

Highlights

- SYR1 is a high-affinity systemin receptor and positively regulates SWR
- SYR2 is a low-affinity systemin receptor and negatively regulates SWR
- SYR2 attenuates SWR by outcompeting SYR1 for binding with the co-receptor SERK3a
- The SYR1-SYR2 module opens up avenues for uncoupling growth-defense trade-offs

Authors

Ke Zhou, Fangming Wu, Lei Deng, ..., Gregg A. Howe, Chang-Bao Li, Chuanyou Li

Correspondence

ldeng@sdau.edu.cn (L.D.), lichangbao@nercv.org (C.-B.L.), chuanyouli@sdau.edu.cn (C.L.)

In brief

Zhou et al. report that two antagonistic wound peptide hormone systemin receptors (SYR1 and SYR2) enable plants to integrate the attenuation of wound signaling with its activation. Whereas SYR1 acts as a high-affinity receptor to initiate systemin signaling, SYR2 functions as a low-affinity receptor in signaling attenuation in tomato.

Zhou et al., 2025, Developmental Cell *60*, 1–16
February 24, 2025
https://doi.org/10.1016/j.devcel.2024.11.005

CellPress

Developmental Cell

CellPress
OPEN ACCESS

Article

Antagonistic systemin receptors integrate the activation and attenuation of systemic wound signaling in tomato

Ke Zhou,[1,2,3,9,15] Fangming Wu,[1,2,15] Lei Deng,[1,4,15,*] Yu Xiao,[7,15] Wentao Yang,[1,2,3] Jiuhai Zhao,[6,8] Qinyang Wang,[1,2,3] Zeqian Chang,[1,2,3] Huawei Zhai,[1,5] Chuanlong Sun,[1,5] Hongyu Han,[1,6] Minmin Du,[1,9] Qian Chen,[1,5] Jijun Yan,[2] Peiyong Xin,[2] Jinfang Chu,[2] Zhifu Han,[10] Jijie Chai,[10,11] Gregg A. Howe,[12,13] Chang-Bao Li,[1,4,14,*] and Chuanyou Li[1,2,3,4,5,16,*]

[1]Taishan Academy of Tomato Innovation, Shandong Agricultural University, Tai'an, Shandong 271018, China
[2]Key Laboratory of Seed Innovation, Institute of Genetics and Developmental Biology, Chinese Academy of Sciences, Beijing 100101, China
[3]College of Advanced Agricultural Sciences, University of Chinese Academy of Sciences, Beijing 100049, China
[4]College of Life Sciences, Shandong Agricultural University, Tai'an 271018, China
[5]College of Horticulture Science and Engineering, Shandong Agricultural University, Tai'an 271018, China
[6]College of Agronomy, Shandong Agricultural University, Tai'an, Shandong 271018, China
[7]Beijing Frontier Research Center for Biological Structure, Tsinghua-Peking Joint Center for Life Sciences, Center for Plant Biology, School of Life Sciences, Tsinghua University, Beijing 100084, China
[8]Key Laboratory of Soybean Molecular Design Breeding, Northeast Institute of Geography and Agroecology, Chinese Academy of Sciences, Changchun 130102, China
[9]Beijing Key Laboratory of Growth and Developmental Regulation for Protected Vegetable Crops, College of Horticulture, China Agricultural University, Beijing 100193, China
[10]Westlake Laboratory of Life Sciences and Biomedicine, Hangzhou, Zhejiang 310024, China
[11]School of Life Sciences, Westlake University, Hangzhou 310024, China
[12]Department of Energy-Plant Research Laboratory, Michigan State University, East Lansing, MI 48824, USA
[13]Plant Resilience Institute, Michigan State University, East Lansing, MI 48824, USA
[14]Key Laboratory of Biology and Genetic Improvement of Horticultural Crops (North China), Ministry of Agriculture, Beijing Institute of Vegetable Science, Beijing Academy of Agriculture and Forestry Sciences, Beijing 100097, China
[15]These authors contributed equally
[16]Lead contact
*Correspondence: ldeng@sdau.edu.cn (L.D.), lichangbao@nercv.org (C.-B.L.), chuanyouli@sdau.edu.cn (C.L.)
https://doi.org/10.1016/j.devcel.2024.11.005

SUMMARY

Pattern recognition receptor (PRR)-mediated perception of damage-associated molecular patterns (DAMPs) triggers the first line of inducible defenses in both plants and animals. Compared with animals, plants are sessile and regularly encounter physical damage by biotic and abiotic factors. A longstanding problem concerns how plants achieve a balance between wound defense response and normal growth, avoiding overcommitment to catastrophic defense. Here, we report that two antagonistic systemin receptors, SYR1 and SYR2, of the wound peptide hormone systemin in tomato act in a ligand-concentration-dependent manner to regulate immune homeostasis. Whereas SYR1 acts as a high-affinity receptor to initiate systemin signaling, SYR2 functions as a low-affinity receptor to attenuate systemin signaling. The expression of systemin and SYR2, but not SYR1, is upregulated upon SYR1 activation. Our findings provide a mechanistic explanation for how plants appropriately respond to tissue damage based on PRR-mediated perception of DAMP concentrations and have implications for uncoupling defense-growth trade-offs.

INTRODUCTION

In response to tissue damage caused by chewing insects or necrotrophic pathogens, higher plants activate cellular and molecular reprogramming involved in attacker deterrence, wound healing, and other defense-related processes.[1–10] A fascinating feature of these inducible defenses is their occurrence both locally at the site of wounding and systemically in remote undamaged leaves (systemic wound responses [SWRs]).[11] Wound-inducible defensive proteinase inhibitors (PIs) in tomato (*Solanum lycopersicum*) provide an attractive model system to investigate the mechanism of SWR.[1,2,11] In their pioneer study of wound-induced PI expression half a century ago, Green and Ryan proposed that specific mobile signals generated at the wound site travel throughout the plant and activate defense gene expression in systemic leaves.[11] The discovery of SWR in

Please cite this article in press as: Zhou et al., Antagonistic systemin receptors integrate the activation and attenuation of systemic wound signaling in tomato, Developmental Cell (2024), https://doi.org/10.1016/j.devcel.2024.11.005

tomato spurred remarkable progress in our understanding of systemic wound signaling and other long-distance signaling events in plants.[4,12–14]

Among the well-established intercellular signals promoting SWR are systemin, the first bioactive peptide isolated from plants, and the wound hormone jasmonate (JA).[15,16] Systemin is an 18-amino-acid immunomodulatory peptide cleaved from a precursor protein called prosystemin.[15,17,18] Transgenic tomato plants expressing an antisense *PROSYSTEMIN* (*PRS*) gene lack SWR and were more susceptible to necrotrophic pathogens.[18,19] Conversely, transgenic tomato plants (*35S::PRS*) that overexpress *PRS* constitutively express SWR without wounding and are more resistant to insects.[20] In addition, jasmonate mutants can suppress the constitutive wound signaling phenotype of 35*S::PRS* plants.[21,22] These genetic studies, together with a wealth of other evidence, led to a model in which systemin functions upstream of jasmonate and that these two signals act through a common signaling pathway to regulate SWR.[2,23,24]

Upon its discovery, systemin was initially considered to be the long sought-after systemic wound signal.[2,11,15] However, grafting experiments with tomato mutants defective in jasmonate and/or systemin signaling provided evidence that systemin acts locally at the site of wounding, where it amplifies jasmonate production to threshold levels that are required for the activation of systemic defense responses.[22–27] This proposed mode of action of systemin in the amplification of systemic immunity shares similarities to metazoan cytokines.[28–31] From this perspective, systemin and other related host-derived, damage-associated molecular patterns (DAMPs) may be termed immunomodulatory phytocytokines.[17,28,32–34]

In the current model of systemic wound signaling, cellular damage induces the proteolytic cleavage of prosystemin to produce mature systemin,[35] which then travels to neighboring cells where it is perceived by its putative receptor. Systemin receptor activation triggers a signaling cascade that promotes the production of jasmonate, which, in turn, initiates long-distance signaling and activates the immune transcriptional reprogramming by the master transcription factor MYC2.[5,17,23,36–38] Thus, a linear intracellular signaling pathway from surface-localized pattern recognition receptor (PRR) complex to nuclear-localized transcription factors is thought to execute the activation and amplification of SWR. However, identification of the systemin receptor has proven to be very challenging. Until recently, Wang et al. reported that the tandemly duplicated leucine-rich-repeat receptor-like kinases (LRR-RLKs) systemin receptor 1 and 2 (SYR1 and SYR2) are involved in systemin perception.[39] They showed that SYR1 is a genuine receptor for systemin but did not assign a definitive function to SYR2 and concluded that SYR1 is not decisive for local and SWRs,[39] which contradicts the well-established function of systemin in regulating SWR.

Unlike animals, the sessile lifestyle of plants increases their exposure to physical damage by abiotic and biotic factors. Because sustained activation of wound signaling can inhibit plant growth and fitness, a plant's capacity to attenuate wound signaling must be tightly integrated with the activation of the pathway.[5,40,41] However, the molecular mechanisms responsible for the balance between activation and attenuation remain unknown.

Here, we discovered a mechanism by which two antagonistic systemin receptors act in concert to initiate and attenuate SWR. Multiple lines of evidence suggest that SYR1 functions as a high-affinity receptor that initiates systemin signaling through ligand-induced heteromerization with its co-receptor somatic embryogenesis receptor kinase 3a (SERK3a), whereas SYR2 functions as a low-affinity receptor that attenuates systemin signaling by outcompeting SYR1 for binding to SERK3a. Wounding specifically upregulates the expression of *PRS* and *SYR2*, but not SYR1, through the master transcription factor MYC2. Our findings highlight how plants fine-tune the wound response based on receptor-mediated perception of variable concentrations of a damage-induced immunomodulatory phytocytokine.[42–44]

RESULTS

SPR1-dependent systemin signaling is required for resistance to *Botrytis cinerea* and *Spodoptera exigua*

The tomato *suppressor of prosystemin-mediated responses1* (*spr1*) mutant was previously identified as lacking prosystemin-mediated responses.[27] In contrast to jasmonate mutants, which are defective in wound-inducible local and systemic defense responses,[21,22] *spr1* mutants lacked a SWR yet maintained an intermediate local wound response (Figure 1A). Consistent with our previous observation that *spr1* defines a signaling step that couples systemin perception to activation of jasmonate signaling,[27] *spr1* plants were insensitive to systemin but were fully responsive to exogenous jasmonate, as assessed by expression of a PI marker gene (*PI-II*) and root growth inhibition assays (Figures 1B–1E).

The deficiency of *spr1* plants to express defensive PI-II in response to wounding and systemin suggested that the mutant might be compromised in resistance to chewing insects. To test this, we examined the performance of *Spodoptera exigua*, a globally significant agricultural pest,[3] in feeding assays with *spr1* mutants and *35S::PRS* plants. The weight gain of larvae fed with *spr1* leaves was significantly greater than that of larvae fed with wild-type (WT) leaves (Figure 1F). By contrast, the weight gain of larvae fed with *35S::PRS* leaves was significantly lower than that of larvae fed with WT leaves (Figure 1F). Next, we examined the performance of *spr1* mutants in infection assays with *Botrytis cinerea*, a widespread fungal pathogen with a necrotrophic lifestyle.[9,45] In line with previous observation that systemin is involved in tomato resistance to *B. cinerea*,[19] *B. cinerea*-induced necrotic lesions on *35S::PRS* leaves were significantly smaller than those on WT leaves (Figure 1G). By contrast, *B. cinerea*-induced necrotic lesions on *spr1-1* and *spr1-2* leaves were significantly larger than those on WT leaves (Figure 1G). Collectively, these results support that SPR1-dependent systemin signaling is required for plant resistance to both chewing insects and necrotrophic pathogens.

SPR1 encodes the systemin receptor SYR1 that positively regulates systemin signaling and SWR

We leveraged the systemin insensitivity of *spr1-1* to support map-based identification of the *SPR1* gene. We screened a segregating population for the systemin-mediated root growth inhibition phenotype and performed bulk population sequencing

Please cite this article in press as: Zhou et al., Antagonistic systemin receptors integrate the activation and attenuation of systemic wound signaling in tomato, Developmental Cell (2024), https://doi.org/10.1016/j.devcel.2024.11.005

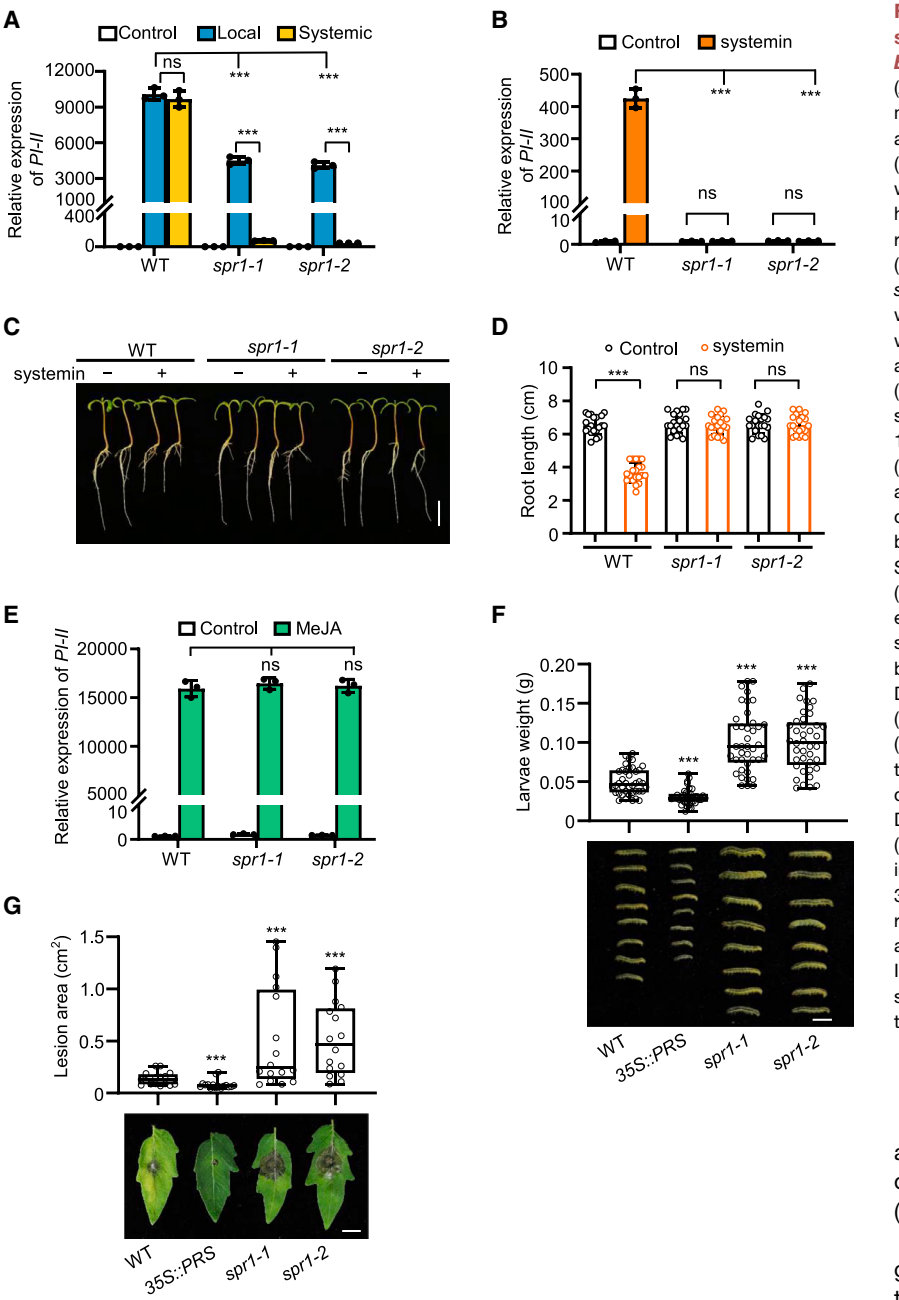

Figure 1. *SPR1*-dependent systemin signaling is required for resistance to *B. cinerea* and *S. exigua*

(A) Wound-induced *PI-II* expression in WT and *spr1* mutants. 18-day-old seedlings were wounded, and damaged (local) leaves and undamaged (systemic) leaves were harvested 12 h after wounding. Leaves of undamaged seedlings were harvested as control. Data are mean ± SD, $n = 3$ repeats.

(B) Systemin-induced *PI-II* expression in WT and *spr1* mutants. 18-day-old seedlings were treated with or without 100 nM systemin. *PI-II* expression was measured 12 h after systemin treatment. Data are mean ± SD, $n = 3$ repeats.

(C) Image of 5-day-old WT, *spr1-1*, and *spr1-2* seedlings grown on medium with or without 100 nM systemin. Scale bar, 2 cm.

(D) Systemin-induced root growth inhibition in WT and *spr1* mutants. Seedlings were grown on medium with or without 100 nM systemin for 5 days before root length was measured. Data are mean ± SD, $n = 20$ seedlings.

(E) Methyl jasmonate (MeJA)-induced *PI-II* expression in WT, *spr1-1*, and *spr1-2*. 18-day-old seedlings were exposed to MeJA vapor for 12 h before sampling for gene expression analysis. Data are mean ± SD, $n = 3$ repeats.

(F) Average weight (top) and representative image (bottom) of *S. exigua* larvae after 4-day feeding trials on leaves of indicated genotypes. Each circle dot represents the weight of an individual larva. Data are mean ± SD, $n = 40$ larvae. Scale bar, 1 cm.

(G) Average lesion area (top) and representative image (bottom) of *B. cinerea*-inoculated leaves at 3 days after inoculation (DAI). Each circle dot represents the lesion area of an individual leaf. Data are mean ± SD, $n = 16$ leaves. Scale bar, 1 cm.

In (A), (B), and (D)–(G), the error bars represent standard deviation (SD). ***$p < 0.001$ (Student's t test); ns, not significant.

on DNA pools obtained from F2 individuals with either the *spr1-1* or WT phenotype. Single-nucleotide polymorphism (SNP) comparison between the two DNA pools located the target gene to a heterochromatin region on chromosome 3 (Figure 2A). Within the *SPR1* mapping interval, we identified two tandemly duplicated LRR-RLK genes (Figures 2A, 2B, and S1A), which encode SYR1 (Solyc03g082470) and SYR2 (Solyc03g082450).[39] Sequencing the genomic loci of *SYR1* and *SYR2* in *spr1-1* and *spr1-2* revealed that the former allele contained a T2854A mutation of *SYR1*, which leads to a Y952N amino acid substitution in the kinase domain of the SYR1 protein, whereas *spr1-2* contained a G710A mutation in *SYR1*, which results in a C237Y amino acid substitution in the LRR domain of the predicted SYR1 protein (Figures 2B and S1A).

To verify that *SYR1* is the causative gene for the systemin-insensitive phenotype, the WT *SYR1* genomic DNA with its native promoter was introduced into the *spr1-1* mutant. The resulting transgenic plants were fully responsive to exogenous systemin and exhibited a local and SWR that was indistinguishable from that of WT plants (Figures 2C–2E and S1B). We then generated *SYR1*-overexpression (*SYR1-OE*) plants (Figure S1C) and CRISPR-Cas9-mediated null alleles (*syr1*) of *SYR1* (Figure S1D). Systemin- and wound-triggered responses of *syr1* plants were similar to the *spr1-1* mutant, whereas systemin- and wound-triggered responses of *SYR1-OE* plants were significantly increased compared with the WT (Figures 2F and 2G). Collectively, these results demonstrate that *SPR1* encodes the systemin receptor SYR1, which positively regulates both systemin signaling and SWR.

Please cite this article in press as: Zhou et al., Antagonistic systemin receptors integrate the activation and attenuation of systemic wound signaling in tomato, Developmental Cell (2024), https://doi.org/10.1016/j.devcel.2024.11.005

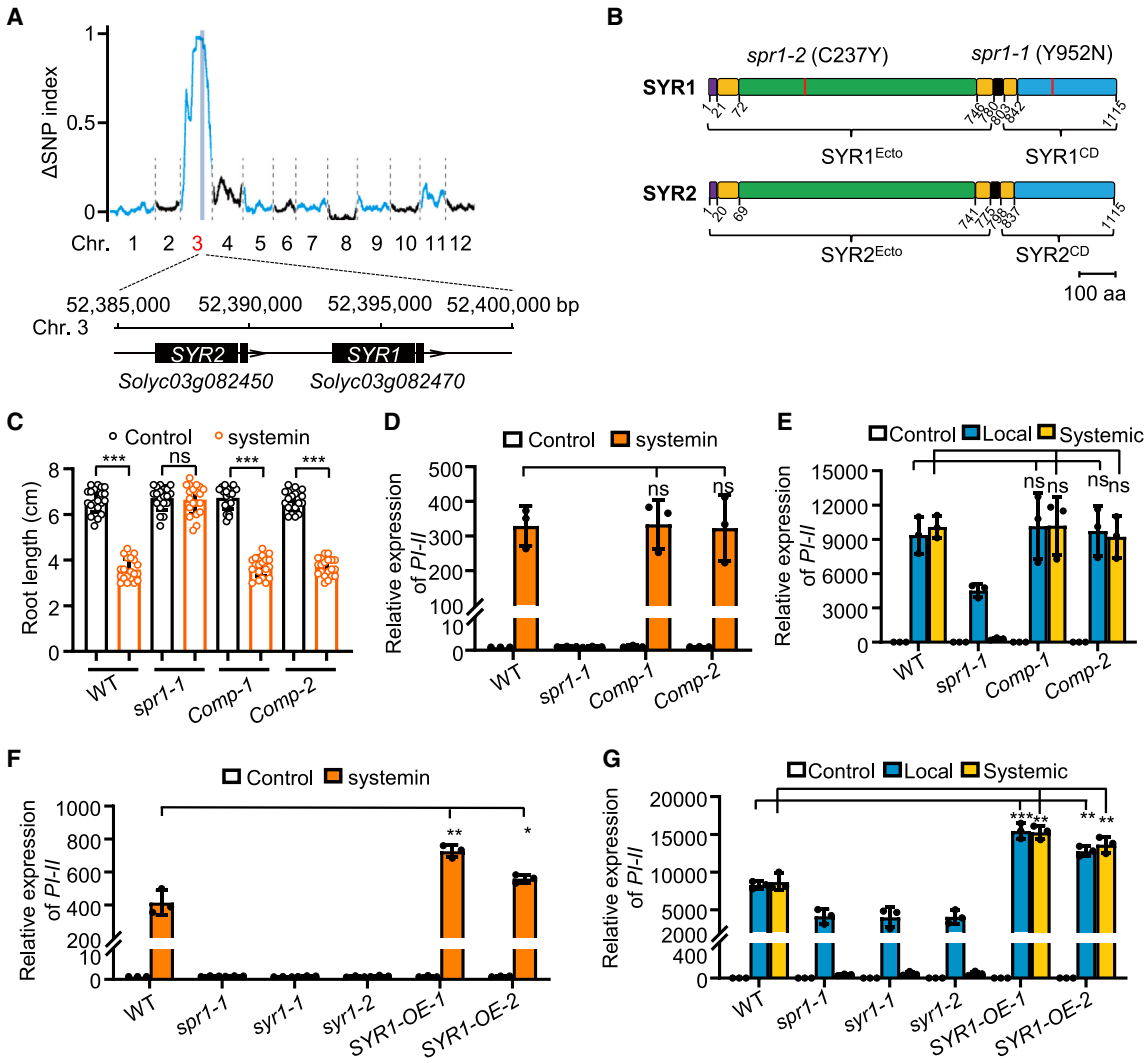

Figure 2. *SPR1* encodes the systemin receptor SYR1 that positively regulates systemin signaling and SWR

(A) Mapping-by-sequencing of the *SPR1* gene. Shown was ΔSNP index of all 12 chromosomes between the two DNA pools.

(B) Schematic domain architecture of SYR1 and SYR2. Purple boxes indicate the signal peptide; green boxes indicate the LRR domain; black boxes indicate the transmembrane domain; blue boxes indicate kinase domain; red lines indicate mutations in *spr1-1* and *spr1-2*. Ecto, ectodomain; CD, cytoplasmic domain.

(C) Systemin-induced root growth inhibition of indicated genotypes. Seedlings were grown on medium with or without 100 nM systemin for 5 days before root length was measured. Data are mean ± SD, $n = 20$ seedlings.

(D–G) Systemin- (D) and (F) and wound-induced (E) and (G) *PI-II* expression in the indicated genotypes. 18-day-old seedlings were treated with 100 nM systemin (D) and (F) or wounded (E) and (G), and seedlings were harvested 12 h after treatment. Data are mean ± SD, $n = 3$ repeats.

In (C)–(G), the error bars represent SD. $^{*}p < 0.05$, $^{**}p < 0.01$, $^{***}p < 0.001$ (Student's t test); ns, not significant.

See also Figure S1.

SYR2 negatively regulates systemin signaling and SWR

Previous studies showed that SYR1 is a genuine receptor for systemin but did not assign a definitive function to SYR2.[39] We explored this question by generating null mutants (*syr2*) of *SYR2* (Figure S2A) as well as *SYR2*-overexpression (*SYR2-OE*) plants (Figure S2B). Surprisingly, we observed that systemin-induced *PI-II* expression was increased in *syr2* plants (Figure 3A) but was decreased in *SYR2-OE* plants (Figure 3B) as compared with the WT, suggesting that SYR2 negatively regulates systemin signaling. To substantiate this observation, we examined the contribution of SYRs to systemin-induced production of reactive oxygen species (ROS). In line with previous studies,[39] WT plants treated with systemin displayed a rapid (within 5 min) and transient ROS burst (Figure 3C). That the systemin-induced ROS burst was nearly abolished in *syr1* plants confirmed that SYR1 positively regulates systemin signaling. However, the systemin-induced ROS burst was significantly elevated in *syr2* plants (Figure 3C), consistent with the hypothesis that SYR2 negatively regulates systemin signaling. We also found that wound-induced *PI-II* expression was significantly increased in *syr2* plants (Figure 3D) but was decreased in *SYR2-OE* plants (Figure 3E) compared with the WT, further supporting that SYR2 negatively regulates SWR.

Please cite this article in press as: Zhou et al., Antagonistic systemin receptors integrate the activation and attenuation of systemic wound signaling in tomato, Developmental Cell (2024), https://doi.org/10.1016/j.devcel.2024.11.005

CellPress
OPEN ACCESS

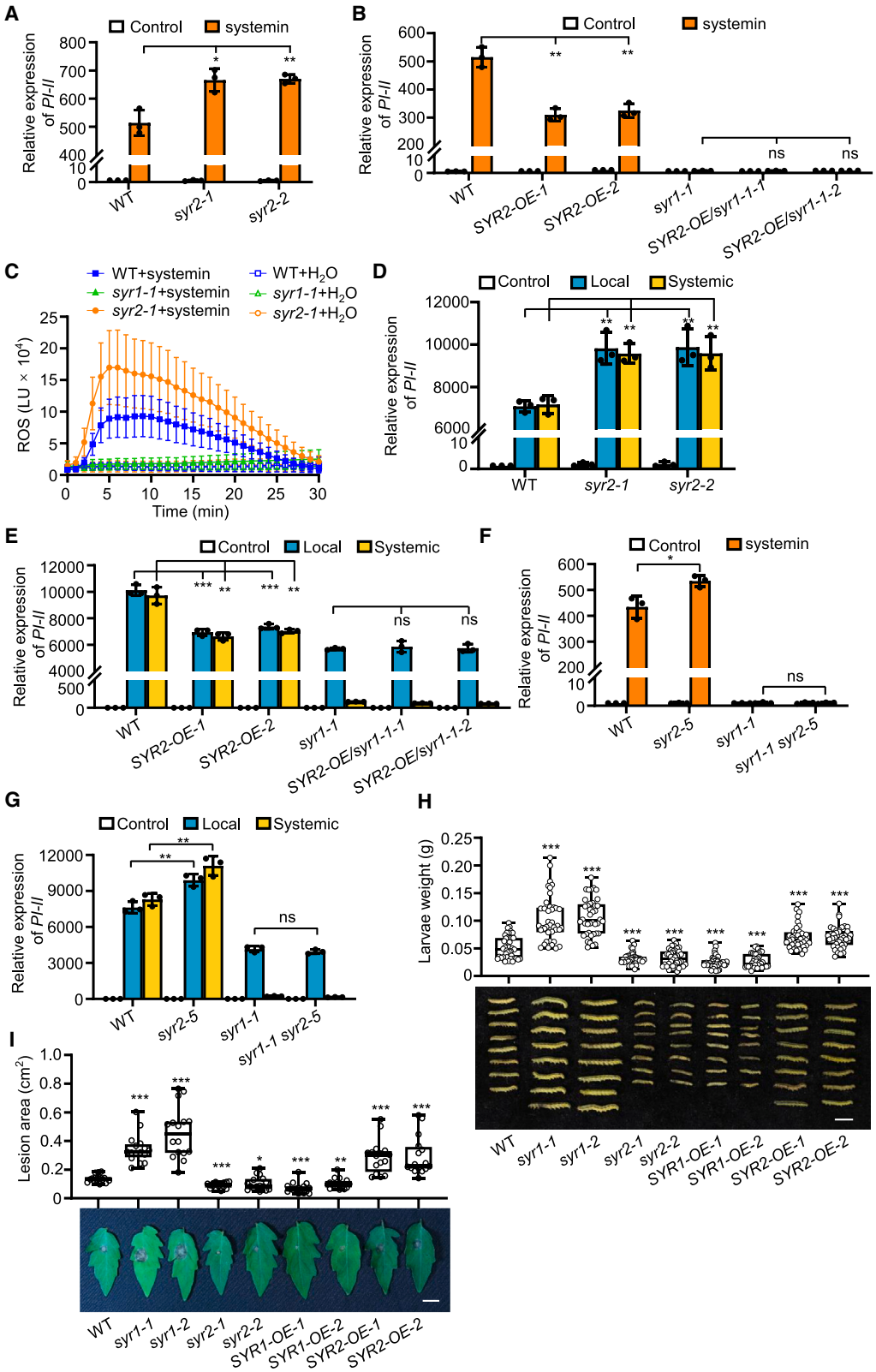

Figure 3. SYR2 negatively regulates systemin signaling and SWR

(A and B) Systemin-induced *PI-II* expression in indicated genotypes. 18-day-old seedlings were treated with or without 100 nM systemin. *PI-II* expression was measured 12 h after treatment. Data are mean ± SD, *n* = 3 repeats.

(legend continued on next page)

That SYR1 and SYR2 antagonistically regulate systemin signaling and SWR prompted us to investigate their genetic interactions. To this end, we generated *SYR2-OE* plants in the *syr1-1* background (Figure S2B) and *syr1 syr2* double mutants (Figure S2C). Systemin- and wounding-triggered responses of *SYR2-OE/syr1-1* plants (Figures 3B and 3E) and *syr1 syr2* (Figures 3F and 3G) resembled *syr1* plants, suggesting that the function of SYR2 depends on SYR1.

To further understand the biological function of these antagonistic SYRs, we performed *S. exigua* feeding assays and *B. cinerea* infection assays with *syr* mutants and *SYR-OE* plants. The weight gain of larvae fed with *syr1* leaves was significantly greater than that of larvae fed with WT leaves, whereas the weight gain of larvae fed with *SYR1-OE* leaves was significantly lower than that of larvae fed with WT leaves (Figure 3H). By contrast, the weight gain of larvae fed with *syr2* leaves was significantly lower than that of larvae fed with WT leaves, whereas the weight gain of larvae fed with *SYR2-OE* leaves was significantly higher than that of larvae fed with WT leaves (Figure 3H). In parallel pathogen infection assays, *B. cinerea*-induced lesions on *syr1* and *SYR2-OE* leaves were significantly larger than those on WT leaves (Figure 3I). By contrast, *B. cinerea*-induced lesions on *SYR1-OE* and *syr2* leaves were significantly smaller than those on WT leaves (Figure 3I). Collectively, these results indicate that, whereas SYR1 positively regulates plant resistance against herbivorous insects and necrotrophic pathogens, SYR2 plays a negative role in regulating these responses.

The systemin-binding affinity of SYR2 is much lower than SYR1

Pull-down assays using *Nicotiana benthamiana* cell-expressed SYR ectodomains (SYR^{Ectos}) and biotinylated systemin showed that both SYRs interacted with systemin (Figure 4A). However, the ability of SYR2 to interact with biotinylated systemin was reproducibly weaker than that of SYR1 (Figure 4A). To further compare the capability of SYRs to bind systemin, we performed peptide competition experiments with *N. benthamiana* cell-expressed SYR^{Ectos} and systemin labeled with an acridinium ester (acri-systemin). Acri-systemin was widely used for sensitive detection of the active peptide via chemiluminescence.[39] For these experiments, SYR^{Ecto} immunoprecipitates were incubated with 10 nM acri-systemin to determine total binding or with 10 nM acri-systemin and a 10,000-fold excess of unlabeled systemin to assay for non-specific binding, respectively (Figure 4B). Specific binding (total binding minus non-specific binding) of acri-systemin to $SYR2^{Ecto}$ was shown to be much lower than that to $SYR1^{Ecto}$ (Figure 4B), corroborating that the systemin binding affinity of SYR2 is much lower than SYR1.

Further, dose-response studies revealed that unlabeled systemin, but not the bacterial flagellin epitope flg22, effectively competed the binding of acri-systemin to $SYR1^{Ecto}$, with a half-maximal competition (IC_{50}) at ~18 nM (Figure 4C). We also tested the competition effect of $systemin^{1-14}$, a systemin antagonist that comprises the N-terminal 14 amino acids.[46] Results showed that $systemin^{1-14}$ competed the binding of acri-systemin to $SYR1^{Ecto}$ with an IC_{50} of ~220 nM (Figure 4C). In parallel experiments, systemin and $systemin^{1-14}$ competed the binding of acri-systemin to $SYR2^{Ecto}$ with IC_{50} of ~2.5 and ~15.2 μM, respectively (Figure 4D), whereas flg22 did not show detectable competition effect (Figure 4D). Collectively, our peptide competition experiments indicate that the systemin-binding affinity of SYR2 is much lower than SYR1.

To distinguish the responsiveness of SYR1 and SYR2 to systemin, we assessed their contribution to several of the systemin-triggered early signaling events.[2] When ectopically expressed in *N. benthamiana*, a species that lacks the systemin perception system,[39] *SYR1* was responsive to systemin, exhibiting rapid induction of a ROS burst (Figure 4E). By comparison, the responsiveness of *SYR2*-expressing leaves was delayed and weaker than leaves expressing *SYR1* (Figure 4E). Dose-response studies showed that *N. benthamiana* leaves expressing *SYR1* conferred responsiveness to subnanomolar concentrations of systemin, resulting in half-maximal stimulation (EC_{50}) at ~0.06 nM systemin (Figure 4F). Leaves expressing *SYR2* were less sensitive and responded with an EC_{50} of >20 nM systemin (Figure 4F), indicating that the systemin-binding affinity of SYR2 is much lower than SYR1.

We then used a protoplast-based reporter assay to examine whether the SYRs can mediate systemin-induced expression of *FRK1*, an early marker gene for PRR activation.[39,47] *Arabidopsis thaliana* protoplasts transfected with *SYR1* showed marked induction of *FRK1* promoter-luciferase reporter (*pFRK1::LUC*) in response to systemin, whereas those transfected with *SYR2* only displayed marginal reporter induction (Figure 4G), confirming that the systemin responsiveness of SYR2 is lower than SYR1. In this assay, systemin-dependent induction of *pFRK1::LUC* occurred with an EC_{50} of ~0.05 nM with SYR1 and more than 1 μM with SYR2 (Figure 4H). Collectively, these observations are consistent with a previous report showing that SYR1 exhibits high-affinity systemin binding[39] and support a scenario in which both SYRs are systemin receptors, with SYR2 having a markedly lower affinity for the systemin ligand compared with SYR1.

(C) Systemin-induced ROS burst in indicated genotypes. Leaves from 18-day-old seedlings were treated with or without 100 nM systemin. ROS production was detected by luminometer over 30 min. LU, light unit. Data are mean ± SD, $n = 8$ leaf discs. Experiments were repeated three times with similar results.
(D and E) Wound-induced *PI-II* expression in the indicated genotypes. 18-day-old seedlings were wounded, and damaged (local) leaves and undamaged (systemic) leaves were harvested 12 h after wounding for RNA isolation. Leaves of undamaged seedlings were harvested as control. Data are mean ± SD, $n = 3$ repeats.
(F and G) Systemin- (F) and wound-induced (G) *PI-II* expression in the indicated genotypes. 18-day-old seedlings were treated with 100 nM systemin (F) or wounded (G), seedlings were harvested 12 h after treatment. Data are mean ± SD, $n = 3$ repeats.
(H) Average weight (top) and representative image (bottom) of *S. exigua* larvae after 4-day feeding trials on leaves of indicated genotypes. Each circle dot represents the weight of an individual larva. Data are mean ± SD, $n = 40$ larvae. Scale bar, 1 cm.
(I) Average lesion area (top) and representative image (bottom) of *B. cinerea*-inoculated leaves at 3 DAI. Each circle dot represents the lesion area of an individual leaf. Data are mean ± SD, $n = 16$ leaves. Scale bar, 1 cm.
In (A), (B), and (D)–(I), the error bars represent SD. $^{*}p < 0.05$, $^{**}p < 0.01$, $^{***}p < 0.001$ (Student's t test); ns, not significant.
See also Figure S2.

Please cite this article in press as: Zhou et al., Antagonistic systemin receptors integrate the activation and attenuation of systemic wound signaling in tomato, Developmental Cell (2024), https://doi.org/10.1016/j.devcel.2024.11.005

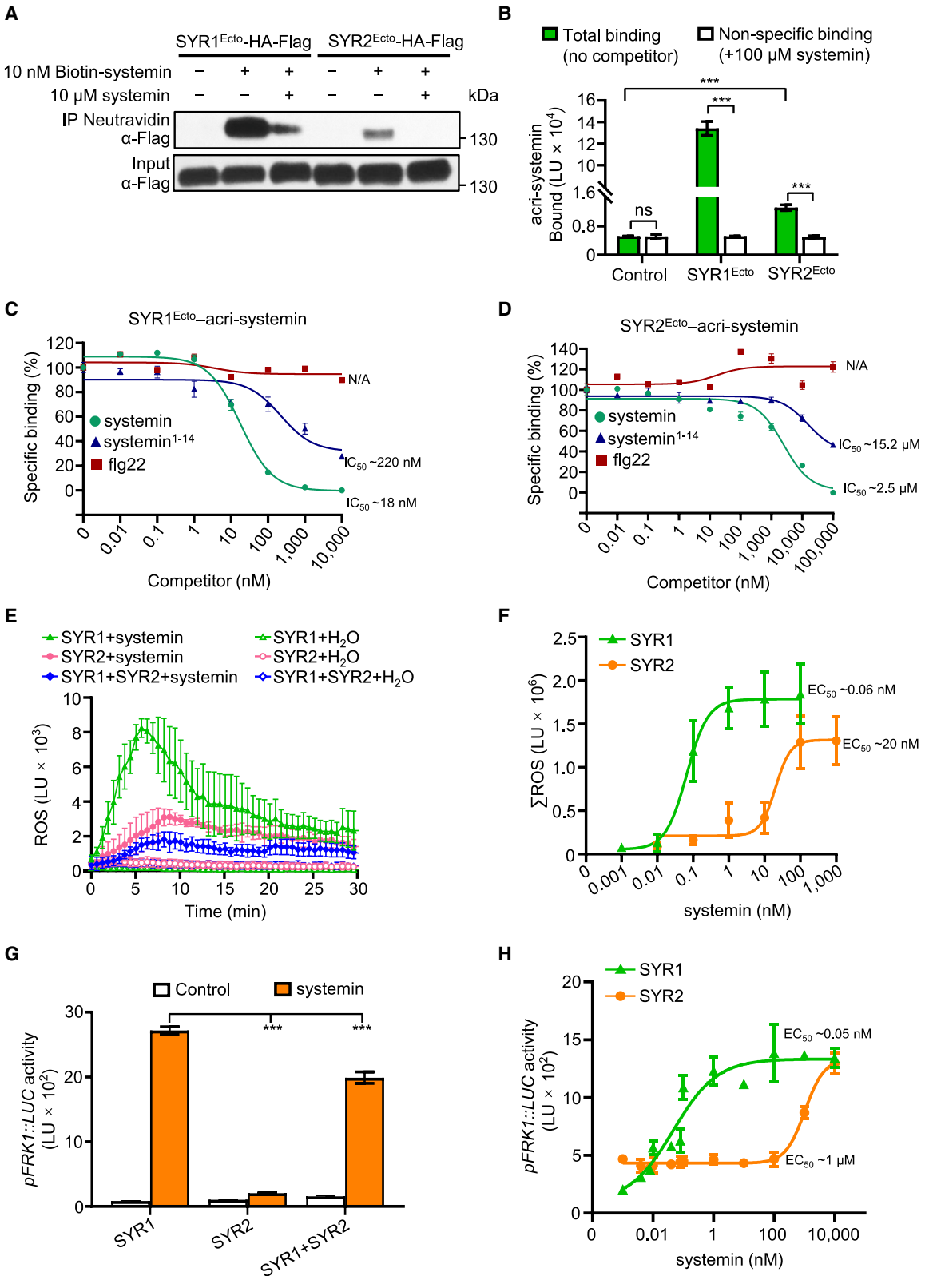

(legend on next page)

Please cite this article in press as: Zhou et al., Antagonistic systemin receptors integrate the activation and attenuation of systemic wound signaling in tomato, Developmental Cell (2024), https://doi.org/10.1016/j.devcel.2024.11.005

SYR2 antagonizes SYR1-mediated systemin signaling

In vitro phosphorylation assays showed that the cytoplasmic domains (CDs) of both SYRs displayed kinase activity (Figure 5A). Mutations in the putative ATP-binding sites[48] of the kinase domain (K872E in SYR1 and K867E in SYR2) abolished their kinase activity (Figure 5A). The Y952N substitution encoded by the *spr1-1* allele also caused loss of kinase activity (Figure 5A). When transiently expressed in *N. benthamiana*, the kinase activity of SYR1 was increased after systemin elicitation (Figure 5B), whereas that of SYR2 was only mildly induced by systemin (Figure 5B), indicating that systemin triggers weaker kinase activity on SYR2 than SYR1. Moreover, SYR2 attenuated the capability of SYR1 to mediate systemin-induced ROS production (Figure 4E) and *pFRK1::LUC* expression (Figure 4G), suggesting that SYR2 antagonizes SYR1 in mediating these systemin responses.

Next, we assessed the contribution of SYRs to systemin-induced mitogen-activated protein kinase (MAPK) activation.[2,49] Systemin-induced MPK3/6 phosphorylation in *SYR2*-expressing *N. benthamiana* leaves was much lower than that in *SYR1*-expressing leaves (Figure 5C), confirming that the systemin-dependent signaling capacity of SYR2 is weaker than SYR1. In these assays, SYR2 attenuated SYR1-mediated MPK3/6 phosphorylation (Figure 5D), corroborating that SYR2 antagonizes SYR1-mediated systemin signaling.

At 30 min after systemin treatment, MPK3/6 phosphorylation was significantly increased in WT seedlings (Figure 5E). This systemin-induced MPK3/6 phosphorylation was decreased in *syr1* but was enhanced in *SYR1-OE* plants (Figure 5E). By contrast, systemin-induced MPK3/6 phosphorylation was enhanced in *syr2* but was impaired in *SYR2-OE* plants (Figure 5E), suggesting that SYRs antagonistically regulate systemin-induced MAPK activation. Moreover, both *syr1 syr2* and *SYR2-OE/syr1-1* plants resembled *syr1* plants in exhibiting diminished MPK3/6 phosphorylation in response to systemin (Figure 5E), suggesting that the function of SYR2 depends on SYR1. Together, these results support the notion that SYR2 antagonizes SYR1-mediated systemin signaling in a SYR1-dependent manner.

SYR2 competes with SYR1 for binding to the co-receptor SERK3a

To understand how SYR2 antagonizes SYR1-mediated systemin signaling, we set out to identify their SERK co-receptors. SERKs have been extensively demonstrated to function as co-receptors of multiple LRR-RLKs, which are key and convergent modules in diverse signaling pathways governing plant growth, cell differentiation, and immunity.[43,44] Among the *SERK* co-receptor genes in tomato,[42] CRISPR-Cas9-mediated mutation of *SERK3a*, but not *SERK3b*, led to compromised systemin and SWRs as assessed by *PI-II* expression (Figures 6A, 6B, and S3A–S3D). These data suggested that SERK3a may function as a co-receptor involved in systemin signaling. Indeed, co-immunoprecipitation (coIP) assays using HA-FLAG-tagged SYR1 (SYR1-HA-FLAG) and SYR2-HA-FLAG expressed in *N. benthamiana* showed that both SYRs interacted with SERK3a-myc in a systemin-dependent manner (Figure 6C).

Dose-response assays showed that <1 nM systemin was sufficient to promote interaction between SYR1-HA-FLAG and SERK3a-myc, whereas 50-fold higher concentrations of systemin were required to promote SYR2-HA-FLAG-SERK3a-myc interaction (Figure 6C). This finding is consistent with a lower systemin-binding affinity of SYR2 relative to SYR1.

To test whether and how SYR2 competes with SYR1 for SERK3a binding, *N. benthamiana* leaves coexpressing SYR1-HA-FLAG, SERK3a-myc, and a chemical inducible SYR2-GFP construct[50] were infiltrated with increasing concentrations of estradiol to induce the expression of SYR2-GFP. CoIP results indicated that the systemin-induced capability of SYR1-HA-FLAG to interact with SERK3a-myc was gradually weakened by increasing amounts of SYR2-GFP (Figure 6D), suggesting that SYR2 acts in a dose-dependent manner to compete with SYR1 for SERK3a binding. We also found that SYR2-HA-FLAG did not show interaction with SERK3a-myc and had a negligible effect on SYR1-GFP-SERK3a-myc interaction in the presence of 1 nM systemin, whereas a comparable amount of SYR2-HA-FLAG showed strong interaction with SERK3a and effectively impaired SYR1-GFP-SERK3a-myc interaction in the presence of 100 nM systemin (Figure 6E). Microscale thermophoresis (MST) analysis showed that systemin-dependent $SYR1^{Ecto}$-$SERK3a^{Ecto}$ and $SYR2^{Ecto}$-$SERK3a^{Ecto}$ interaction displayed a K_d of 3.04 and 2.60 μM, respectively (Figure 6F), suggesting that the systemin-dependent binding affinity of SYR2 to SERK3a is comparable to SYR1. Collectively, these results support a role for SYR2 in negative regulation of systemin signaling by interfering with ligand-stimulated formation of an SYR1-SERK3a complex.

Figure 4. SYR1 and SYR2 show distinct systemin-binding affinity

(A) Pull-down assay between HA-FLAG-tagged SYR^{Ectos} with biotinylated systemin. $SYR1^{Ecto}$-HA-FLAG and $SYR2^{Ecto}$-HA-FLAG purified from *N. benthamiana* leaves were incubated with biotinylated systemin. After being pulled down with streptavidin magnetic beads, the bound and input proteins were detected with an anti-FLAG antibody.

(B) Binding of acri-systemin (10 nM) in the absence (total binding) or presence of 100 μM unlabeled systemin (non-specific binding) to immunoprecipitates from *N. benthamiana* leaves expressing $SYR1^{Ecto}$-HA-FLAG or $SYR2^{Ecto}$-HA-FLAG. $SYR1^{Ecto}$-HA-FLAG or $SYR2^{Ecto}$-HA-FLAG purified from *N. benthamiana* leaves was incubated with 10 nM acri-systemin peptide in the presence or absence of 100 μM unlabeled systemin as a competitor. Controls show binding to leaf material from non-transformed *N. benthamiana*. Data are mean ± SD, $n = 3$ repeats. LU, light unit.

(C and D) Competitive binding assays with SYR1 (C) or SYR2 (D) and various concentrations of different competitors indicated. $SYR1^{Ecto}$-HA-FLAG or $SYR2^{Ecto}$-HA-FLAG purified from *N. benthamiana* leaves was incubated with 10 nM acri-systemin and indicated concentrations of systemin, $systemin^{1-14}$, or flg22 as competitors. The signal detected from samples without competitors was defined as 100% binding. Data are mean ± SD, $n = 3$ repeats. N/A, not applicable.

(E and F) Systemin-induced ROS production. *N. benthamiana* leaves transfected with indicated constructs were treated with 100 nM systemin (E) or indicated concentrations of systemin (F). ROS production was calculated at indicated time (E) or integral over 30 min (F). Data are mean ± SD, $n = 6$ leaf discs. Experiments were repeated three times with similar results.

(G and H) Systemin-induced *pFRK1::LUC* expression in *A. thaliana* protoplasts. Protoplasts were transfected with *pFRK1::LUC* along with indicated constructs. After being induced with 100 nM (G) or indicated concentrations (H) of systemin for 3 h, the luciferase activities were measured. Data are mean ± SD, $n = 3$ repeats. In (B) and (G), the error bars represent SD. ***$p < 0.001$ (Student's t test); ns, not significant.

Please cite this article in press as: Zhou et al., Antagonistic systemin receptors integrate the activation and attenuation of systemic wound signaling in tomato, Developmental Cell (2024), https://doi.org/10.1016/j.devcel.2024.11.005

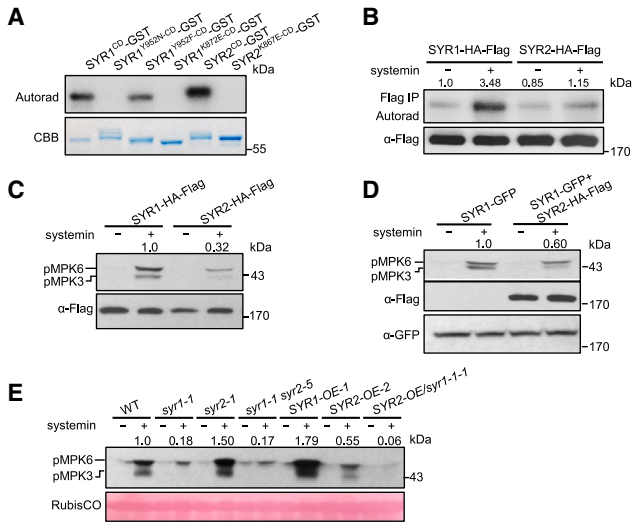

Figure 5. SYR2 antagonizes SYR1-mediated systemin signaling

(A) Autophosphorylation of indicated recombinant proteins expressed in *E. coli*. The purified recombinant proteins were incubated in protein kinase buffer with [γ-^{32}P]ATP and separated by SDS-PAGE gel. The autoradiograph of the gel was shown in the upper panel, and the CBB-stained proteins were shown in the lower panel. CD, cytoplasmic domain. CBB, Coomassie brilliant blue staining.

(B) Systemin-induced autophosphorylation of SYR1 and SYR2. *N. benthamiana* leaves expressing indicated constructs were treated with 100 nM systemin for 20 min before autophosphorylation assays. The autoradiograph of the gel was shown in the upper panel, and the input proteins were detected with an anti-FLAG antibody. Numbers indicate band intensity normalized to SYR1-HA-FLAG without systemin.

(C and D) Systemin-induced MPK3/6 phosphorylation in *N. benthamiana* leaves. *N. benthamiana* leaves expressing indicated constructs were treated with 100 nM systemin for 20 min before immunoblot with anti-pERK antibody. Input proteins are shown with immunoblotting. Numbers indicate arbitrary densitometry units of pMPK3/6 normalized to SYR1-HA-FLAG (C) or SYR1-GFP (D).

(E) Systemin-triggered MPK3/6 activation in tomato seedlings. 18-day-old seedlings of indicated genotypes were treated with 100 nM systemin for 30 min before immunoblot with anti-pERK antibody. Ponceau staining of RuBisCO indicates equal loading. Numbers indicate arbitrary densitometry units of pMPK3/6 normalized to the WT.

To test whether SYR2 negatively regulates responses other than those mediated by the systemin/SYR1 ligand-receptor pair, we examined the responses of *syr2* mutants to flg22, because SERK3a can also be complexed with the LRR-RLK flagellin sensing 2 (FLS2) in a flg22-dependent manner.[42] Results showed that the responsiveness of *syr2* mutants or *syr1* mutants to flg22 was comparable to that of the WT plants in terms of flg22-induced biomass reduction (Figure S3E), ROS production (Figure S3F), and MPK activation (Figure S3G), suggesting that SYR2 specifically competes with SYR1, but not FLS2, for co-receptor binding.

*SYR*s are differentially induced by wounding

Our results suggest that SYR1 and SYR2 likely function in a ligand concentration-dependent manner to initiate and attenuate systemin signaling. If true, we anticipated that wound signaling may dynamically regulate the abundance of three components: SYR1, SYR2, and their ligand systemin. Given the established role of MYC2 in controlling systemin/jasmonate-induced transcriptional reprogramming,[2,5,23,36,41,51] we compared systemin- and wound-induced transcriptional regulation of *SYR1*, *SYR2*, and the systemin precursor gene *PRS*. *SYR2* transcript levels rose rapidly, reaching a peak at 15 min post-systemin feeding and at 60 min post-wounding (Figures 7A and 7B). This pattern of *SYR2* mRNA accumulation is similar to that of *PRS* mRNA, which is also upregulated by wounding.[18] By contrast, we observed only minor (if any) induction of *SYR1* upon systemin or wounding treatments (Figures 7A and 7B). In addition, the protein abundance of PRS (Figures S4A–S4C), systemin (Figure S4D), and the SYR2-HA-FLAG fusion (Figures S4C and S4E) was upregulated upon wounding, while that of the SYR1-HA-FLAG fusion was only mildly induced (Figures S4C and S4F). These results suggest that wounding-triggered transcriptional induction of relevant genes can be translated into protein abundance. Noteworthy, the wound inducibility of *SYR2* and *PRS* was much weaker in *spr1-1* plants and in *MYC2* RNA interference (RNAi) plants (Figures 7C and 7D),[21] revealing that wound-induced transcriptional regulation of *PRS* and *SYR2* requires SYR1-dependent systemin signaling as well as its downstream MYC2-dependent jasmonate signaling.

To understand the transcriptional mechanism through which *SYR1* and *SYR2* are differentially regulated by MYC2-dependent JA signaling, we examined the *SYR* promoters for putative MYC2 binding motifs and identified a G-box-like motif (5′-CACGTT-3′) in *SYR2* promoter and two G-box-like variants (5′-CACTTG-3′) in *SYR1* promoter (Figure 7E). Electrophoretic mobility shift assay indicated that the probe for the *SYR2* promoter (containing the G-box-like motif) showed strong binding affinity for MYC2, whereas the probe for the *SYR1* promoter (containing the G-box-like variant) showed little or no affinity for MYC2 (Figures 7E and 7F). Consistently, chromatin immunoprecipitation-quantitative polymerase chain reaction using *MYC2-GFP* plants[36] and GFP antibody revealed that MYC2-GFP was enriched in the *SYR2* promoter but not the *SYR1* promoter (Figures 7E and 7G). These results collectively suggest that differential binding of MYC2 to the G-box-like motifs in the promoters of *SYR1* and *SYR2* accounts for the distinct transcriptional activation strength of *SYR1* vs. *SYR2* as induced by systemin or wounding.

In summary, our results support a hypothesis that SYR1-iniatiated transcriptional induction of *PRS* and *SYR2* negatively feeds back on SYR1-mediated systemin signaling, thereby illustrating how plant cells precisely (and economically) integrate the attenuation of systemic wound signaling with its initiation. This model predicts that mutations of *SYR1* or *SYR2* could result in distinct effects on plant growth because of the uncoupled activation and attenuation of systemin-dependent SWR. Indeed, when grown on systemin-containing medium, the biomass of *syr2-2* seedlings was more severely inhibited than that of the WT, whereas that of *syr1-1* seedlings was not significantly affected (Figure 7H). When grown in the field, *spr1* and *syr1* plants displayed increased overall growth and enlarged organ size compared with their WT counterparts, whereas *syr2* plants displayed reduced overall growth and organ size (Figures 7I, 7J, and S5), implying that *SYR* genes are promising molecular targets for uncoupling defense-growth trade-offs.

DISCUSSION

The sessile lifestyle of plants makes it impossible to avoid wounding by multiple abiotic and biotic factors, such as wind, rain,

Please cite this article in press as: Zhou et al., Antagonistic systemin receptors integrate the activation and attenuation of systemic wound signaling in tomato, Developmental Cell (2024), https://doi.org/10.1016/j.devcel.2024.11.005

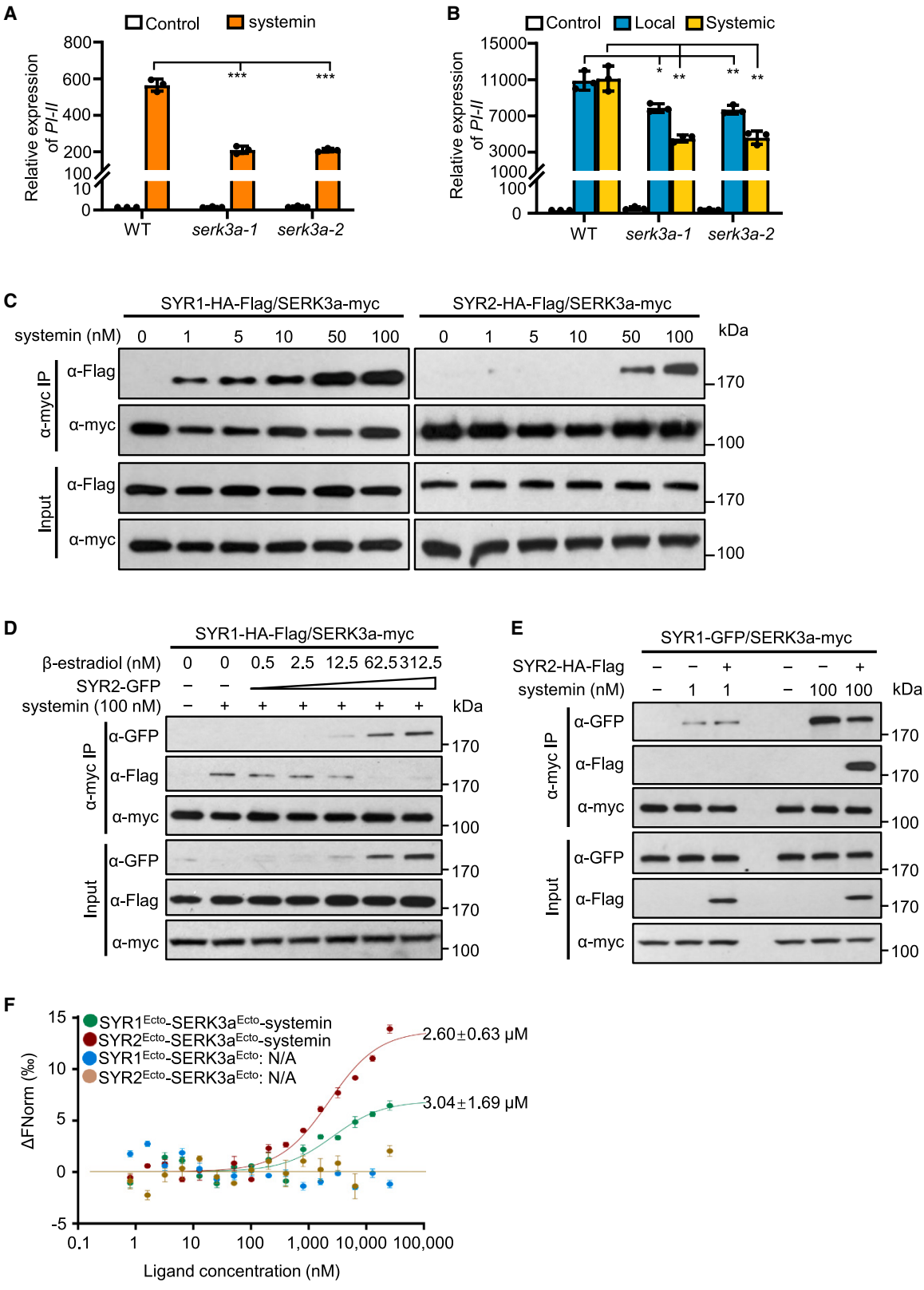

Figure 6. SYR2 competes with SYR1 for binding SERK3a

(A) Systemin-induced *PI-II* expression in WT and *serk3a* mutants. 18-day-old seedlings were treated with or without 100 nM systemin. *PI-II* expression level was measured 12 h after treatment. Data are mean ± SD, *n* = 3 repeats.

(legend continued on next page)

Please cite this article in press as: Zhou et al., Antagonistic systemin receptors integrate the activation and attenuation of systemic wound signaling in tomato, Developmental Cell (2024), https://doi.org/10.1016/j.devcel.2024.11.005

extreme temperatures, as well as herbivores and pathogens. Thus, successful plants must have evolved sophisticated defense mechanisms to cope with those frequently occurring yet rapidly changing cellular damages in an efficient manner. Despite the advances in our understanding of the initiation and amplification of wound signaling, little is known about the attenuation and termination of wound responses and the underlying mechanisms.

Building on our previous success in molecular genetic dissection of systemin/JA-regulated SWR in the model system of tomato, we have identified a mechanism through which antagonistic systemin receptors function in a ligand concentration-dependent manner to couple the attenuation of systemic wound signaling with its activation (Figure 7K). Our data support a model in which cellular damage triggers the production of systemin, which interacts with the high-affinity receptor SYR1, leading to the formation of an active SYR1-SERK3a complex. This complex initiates systemin signaling and subsequently activates MYC2-regulated defense transcriptional reprogramming. In this MYC2-mediated transcriptional regulation, *PRS* and *SYR2*, but not *SYR1*, are transcriptionally induced, which results in an increased relative abundance for both systemin and its low-affinity receptor SYR2. This increase enables SYR2 to outcompete SYR1 for binding with SERK3a, resulting in reduced SYR1 activity and attenuation of the systemin signal (Figure 7K). Thus, SYR1-iniatiated transcriptional induction of *PRS* and *SYR2* exerts negative feedback control on SYR1 to attenuate systemic wound signaling. This receptor competition mechanism for dynamic modulation of the wound response expands current concepts[52,53] of how opposing functions fine-tune peptide-mediated signal transduction in plants.

Notably, as previously described,[39] the SYR1-SYR2 tandem duplication seems to be restricted to the *Solanoideae* subfamily, including tomato, potato, eggplant, and pepper. By contrast, only single SYR-like genes were present in representative species of the sister subfamily *Nicotianoideae* and in other higher plants.[39] It is of significance in future studies to explore the mechanisms through which *Nicotianoideae* plants (contain only single SYR-like genes) integrate the attenuation with activation of systemin-mediated SWR.

Our findings offer explanations for how plants respond appropriately—but not excessively—to wounding. In the face of continuous biotic and abiotic threats that expose plants to tissue damage, this peptide-triggered immune switch may allow an economizing of cellular resources to optimize fitness throughout the life cycle. Our model, however, does not exclude the possibility that other leaf-to-leaf wound response pathways operate in parallel to the systemin pathway, including rapid responses mediated by electrical[13] and calcium signals.[14]

In mammals, trauma induces uncontrolled release of DAMPs (cytokines), which are recognized by PRRs and thereby triggering the activation of inflammatory immune response;[30,54] activation of innate immunity frequently results in post-trauma immune disorders, including exaggerated systemic and organ-specific inflammatory response or immunosuppression, leading to multiple organ failure and death, contributing a leading cause of human death worldwide.[30,54] Despite several features of the plant systemic wound signaling described here are strikingly similar to the inflammatory immune response of animals, plants can appropriately respond to wounding and do not display excessive defense or post-trauma immune dysfunctions. In this perspective, our findings likely provide a mechanistic explanation for how plants appropriately respond to tissue damage based on PRR-mediated perception of injury-induced immunomodulatory phytocytokine concentrations.

Further, emerging evidence has implicated DAMPs as apparent triggers of a battery of wounding-associated complex processes, including wound healing, tissue repair, and organ regeneration.[29,55,56] Indeed, we show here that whereas manipulation of the low-affinity systemin receptor SYR2 favors plant defense, manipulation of the high-affinity systemin receptor SYR1 favors plant growth. In this perspective, future investigations can explore connections between our signaling model and these additional DAMP-associated processes beyond plant defense. In this context, both DAMPs and their receptors can be understood as potential molecular targets for engineering crops with both enhanced fitness and increased yield.

Limitations of the study

We have identified a mechanism through which antagonistic systemin receptors function in a ligand-concentration-dependent manner to couple the attenuation of systemic wound signaling with its activation. Although these findings provide mechanistic explanations for how plants maintain immune homeostasis in response to on-going wounding damage, several open questions remain. First, previous studies have demonstrated that the

(B) Wound-induced *PI-II* expression in WT and *serk3a* mutants. 18-day-old seedlings were wounded. Damaged (local) leaves and undamaged (systemic) leaves were harvested 12 h after wounding for gene expression analysis. Leaves of undamaged seedlings were harvested as control. Data are mean ± SD, $n = 3$ repeats.
(C) SYR1 or SYR2 complexes with SERK3a in a systemin concentration-dependent manner. *N. benthamiana* leaves transfected with indicated constructs were treated with indicated concentrations of systemin for 30 min before IP with anti-myc agarose. SYR1 and SYR2 were detected by immunoblotting with anti-FLAG antibody. Input proteins are shown with immunoblotting.
(D) SYR2 acts in a dose-dependent manner to compete SYR1-SERK3a interaction. *N. benthamiana* leaves coexpressing SYR1-HA-FLAG, SERK3a-myc, and gradients of estradiol-induced SYR2-GFP were treated with 100 nM systemin for 30 min before IP with anti-myc agarose. SYR1 and SYR2 were detected with anti-FLAG and anti-GFP antibody, respectively. Input proteins are shown with immunoblotting.
(E) SYR2 acts in a systemin-concentration-dependent manner to compete SYR1-SERK3a interaction. *N. benthamiana* leaves coexpressing SYR1-GFP, SERK3a-myc, and SYR2-HA-FLAG were treated with 1 nM or 100 nM systemin for 30 min before IP with anti-myc agarose. SYR1 and SYR2 were detected with anti-GFP and anti-FLAG antibody, respectively. Input proteins are shown with immunoblotting.
(F) Quantification of binding affinity of $SYR1^{Ecto}$ and $SYR2^{Ecto}$ with $SERK3a^{Ecto}$ by MST. Data points indicate the difference in normalized fluorescence (%) generated by SYR^{Ectos} or systemin-saturated-SYR^{Ectos} with $SERK3a^{Ecto}$. Data are mean ± SD, $n = 3$ repeats. ΔFNorm, change in fluorescence. N/A, not applicable.
In (A) and (B), the error bars represent SD. $^{*}p < 0.05$, $^{**}p < 0.01$, $^{***}p < 0.001$ (Student's t test).
See also Figure S3.

Please cite this article in press as: Zhou et al., Antagonistic systemin receptors integrate the activation and attenuation of systemic wound signaling in tomato, Developmental Cell (2024), https://doi.org/10.1016/j.devcel.2024.11.005

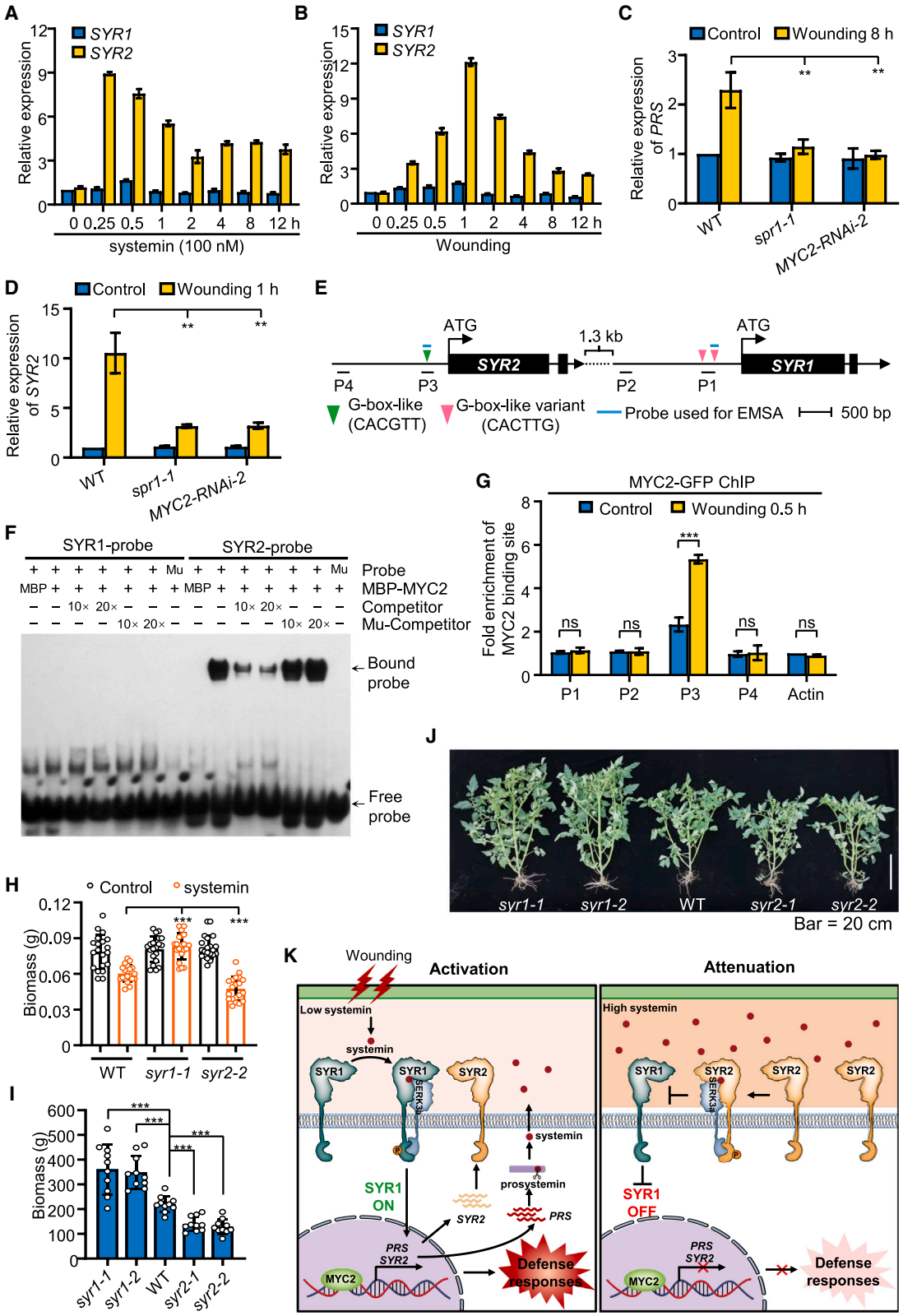

Figure 7. Wounding differentially induces the expression of *SYR1* and *SYR2*

(A and B) Systemin- (A) or wound-induced (B) expression of *SYR1* and *SYR2* of WT seedlings at indicated time. 18-day-old seedlings were treated with 100 nM systemin (A) or wounded (B), then seedlings were harvested at indicated time for gene expression analysis. Data are mean ± SD, *n* = 3 repeats.

(legend continued on next page)

Please cite this article in press as: Zhou et al., Antagonistic systemin receptors integrate the activation and attenuation of systemic wound signaling in tomato, Developmental Cell (2024), https://doi.org/10.1016/j.devcel.2024.11.005

systemin phytocytokine functions upstream of jasmonate and that these two signals act through the same signaling pathway to activate immune transcriptional reprogramming by the master transcription factor MYC2.[2,23,24,36,57] However, the detailed mechanisms by which the systemin-SYR1 ligand-receptor pair relays defense signals (e.g., phosphorylation signaling cascades) to MYC2 need further investigation. Second, although we have elucidated the mechanistic details through which the SYR1-SYR2 negative feedback loop enables plants to integrate the attenuation of systemic wound signaling with its activation, the SYR1-SYR2 tandem duplication appears to be limited to the *Solanoideae* subfamily (e.g., tomato, potato, eggplant, and pepper), and only single SYR-like genes are present in representative species of the sister subfamily *Nicotianoideae* plants.[39] Thus, it is of significance in future studies to explore how *Nicotianoideae* plants, which contain only single SYR-like genes, regulate the activation and attenuation of systemin-mediated SWR. Finally, we exemplified that *syr1* or *syr2* mutations display differential effects on plant growth and organ size, indicating that engineering these antagonistic immune receptors led to significant growth/yield effect. It is now important to identify the specific growth-promoting processes antagonized by the systemin signaling via SYR1, and these studies hold promise to advance on-going efforts of optimizing or uncoupling the growth-defense trade-offs to produce crops with both strong growth and defense traits.[58,59]

RESOURCE AVAILABILITY

Lead contact

Further information and requests for reagents may be directed to and will be fulfilled by the lead contact, Chuanyou Li (chuanyouli@sdau.edu.cn).

Materials availability

All unique reagents generated in this study are available from the lead contact upon completion of a Materials Transfer Agreement.

Data and code availability

- The bulk sequencing data have been deposited in the Genome Sequence Archive (GSA; https://ngdc.cncb.ac.cn/gsa/) at the Beijing Institute of Genomics (BIG) Data Center, Chinese Academy of Sciences, under the accession number GSA: CRA004447.
- Sequence data from this article can be found in the Sol Genomics Network (SGN) or National Center for Biotechnology Information (NCBI) under the following accession numbers: *SYR1* (SGN: Solyc03g082470), *SYR2* (SGN: Solyc03g082450), *SlSERK1* (SGN: Solyc04g072570), *SlSERK3a* (SGN: Solyc10g047140), *SlSERK3b* (SGN: Solyc01g104970), *MYC2* (SGN: Solyc08g076930), *PI-II* (GenBank: K03291.1), *PRS* (SGN: Solyc05g051750), and *ACTIN2* (SGN: Solyc11g005330).
- This paper does not report original code.
- Any additional information required to reanalyze the data reported in this work paper is available from the lead contact upon request.

ACKNOWLEDGMENTS

We thank J. Luo for sharing the pEAQ-HT vector. C.X. Gao, J.-M. Zhou, and J.Y. Li for discussion and critical reading of the manuscript. This work was supported by the National Key R&D Program of China (2022YFD1400800 and 2021YFF1000103), the National Natural Science Foundation of China (32161133018, 31730010, 31991183, and 31970285), the Taishan Industrial Experts Program (tscx202312152), the Natural Science Foundation of Shandong Province (ZR2020JQ12), and the Michigan AgBioResearch Project MICL02278 from Michigan State University (to G.A.H.).

AUTHOR CONTRIBUTIONS

C.L., C.-B.L., L.D., F.W., and K.Z. conceived and designed the overall research with input from G.A.H., and C.L. supervised the project. K.Z., L.D., and F.W. performed most of the experiments. F.W. and W.Y. performed protoplast transient expression assays. K.Z., W.Y., Q.W., M.D., H.H., and L.D. performed genetic analysis, insect feeding trials, and *Botrytis cinerea* inoculation assays. J.Z., K.Z., and Z.C. performed bulk population sequencing and statistical analysis. Y.X. purified proteins from insect cells. Y.X. and F.W. contributed to the MST assays with the help of Z.H. and J. Chai. J.Y., P.X., and J. Chu. performed systemin measurement. K.Z., C.S., Q.C., and H.Z. performed plant material cultivation and management with the help of L.D. G.A.H. provided tomato germplasm. C.L. wrote the paper with input from all authors.

DECLARATION OF INTERESTS

The authors declare no competing interests.

STAR★METHODS

Detailed methods are provided in the online version of this paper and include the following:

- KEY RESOURCES TABLE

(C and D) Wound-induced expression of *PRS* (C) and *SYR2* (D) in the indicated genotypes. 18-day-old seedlings were wounded, and then seedlings were harvested at indicated time for gene expression analysis. Data are mean ± SD, $n = 3$ repeats.
(E) Schematic representation of *SYR1* and *SYR2* showing primers and probes used for chromatin immunoprecipitation (ChIP)-qPCR and electrophoretic mobility shift assay (EMSA). Green and red triangles represent G-box-like or G-box-like variant, respectively. Blue lines represent probes.
(F) EMSA showing that MYC2 binds the G-box-like motif of *SYR2* promoter but not the G-box-like variant of *SYR1* promoter. Labeled probes incubated with the MBP protein and mutated probes incubated with the MBP-MYC2 protein were used as negative controls. 10- and 20-fold excesses of unlabeled or mutated probes were used for competition. Mu, mutated probe in which the G-box-like or G-box-like variant was replaced by 5′-AAAAAA-3′.
(G) ChIP-qPCR showing wound-induced MYC2 enrichment on the chromatin of *SYR1* and *SYR2*. The chromatin of damaged or undamaged *MYC2-GFP* seedlings was immunoprecipitated using anti-GFP antibody, and the immunoprecipitated DNA was quantified by qPCR. The enrichment of target gene promoters was displayed as a percentage of input DNA. *ACTIN2* was used as a nonspecific target. Primers used for PCR amplicons are indicated in (E). Data are mean ± SD, $n = 3$ repeats.
(H) Biomass of 6-day-old seedlings of indicated genotypes grown on medium with or without 100 nM systemin. Data are mean ± SD, $n = 20$ seedlings.
(I and J) Biomass (I) and representative image (J) of 58-day-old field-grown plants of indicated genotypes. Data are mean ± SD, $n = 10$ plants.
(K) Proposed model through which systemin concentration-dependent activation of SYR2 leads to de-activation of SYR1. Damage-induced systemin promotes its high-affinity receptor SYR1 to complex with SERK3a, initiating systemin signaling and activating MYC2-regulated defense transcriptional reprogramming. MYC2-mediated dynamic transcriptional regulation leads to an increased abundance of both systemin and its low-affinity receptor SYR2. This increase enables SYR2 to outcompete SYR1 for binding with SERK3a, resulting in reduced SYR1 activity and attenuation of the systemin signal.
In (C), (D), and (G)–(I), the error bars represent SD. $^{**}p < 0.01$, $^{***}p < 0.001$ (Student's t test); ns, not significant.
See also Figures S4 and S5.

SUPPLEMENTAL INFORMATION

Supplemental information can be found online at https://doi.org/10.1016/j.devcel.2024.11.005.

Received: March 28, 2024
Revised: July 22, 2024
Accepted: November 8, 2024
Published: December 3, 2024

REFERENCES

1. Ryan, C.A., and Pearce, G. (1998). Systemin: a polypeptide signal for plant defensive genes. Annu. Rev. Cell Dev. Biol. *14*, 1–17. https://doi.org/10.1146/annurev.cellbio.14.1.1.
2. Ryan, C.A. (2000). The systemin signaling pathway: differential activation of plant defensive genes. Biochim. Biophys. Acta *1477*, 112–121. https://doi.org/10.1016/s0167-4838(99)00269-1.
3. Howe, G.A., and Jander, G. (2008). Plant immunity to insect herbivores. Annu. Rev. Plant Biol. *59*, 41–66. https://doi.org/10.1146/annurev.arplant.59.032607.092825.
4. Hilleary, R., and Gilroy, S. (2018). Systemic signaling in response to wounding and pathogens. Curr. Opin. Plant Biol. *43*, 57–62. https://doi.org/10.1016/j.pbi.2017.12.009.
5. Howe, G.A., Major, I.T., and Koo, A.J. (2018). Modularity in jasmonate signaling for multistress resilience. Annu. Rev. Plant Biol. *69*, 387–415. https://doi.org/10.1146/annurev-arplant-042817-040047.
6. Erb, M., and Reymond, P. (2019). Molecular interactions between plants and insect herbivores. Annu. Rev. Plant Biol. *70*, 527–557. https://doi.org/10.1146/annurev-arplant-050718-095910.
7. Glazebrook, J. (2005). Contrasting mechanisms of defense against biotrophic and necrotrophic pathogens. Annu. Rev. Phytopathol. *43*, 205–227. https://doi.org/10.1146/annurev.phyto.43.040204.135923.
8. Pieterse, C.M.J., Van der Does, D., Zamioudis, C., Leon-Reyes, A., and Van Wees, S.C.M. (2012). Hormonal modulation of plant immunity. Annu. Rev. Cell Dev. Biol. *28*, 489–521. https://doi.org/10.1146/annurev-cellbio-092910-154055.
9. Bi, K., Liang, Y., Mengiste, T., and Sharon, A. (2023). Killing softly: a roadmap of *Botrytis cinerea* pathogenicity. Trends Plant Sci. *28*, 211–222. https://doi.org/10.1016/j.tplants.2022.08.024.
10. Mengiste, T. (2012). Plant immunity to necrotrophs. Annu. Rev. Phytopathol. *50*, 267–294. https://doi.org/10.1146/annurev-phyto-081211-172955.
11. Green, T.R., and Ryan, C.A. (1972). Wound-induced proteinase inhibitor in plant leaves: a possible defense mechanism against insects. Science *175*, 776–777. https://doi.org/10.1126/science.175.4023.776.
12. Choi, W.G., Hilleary, R., Swanson, S.J., Kim, S.H., and Gilroy, S. (2016). Rapid, long-distance electrical and calcium signaling in plants. Annu. Rev. Plant Biol. *67*, 287–307. https://doi.org/10.1146/annurev-arplant-043015-112130.
13. Mousavi, S.A.R., Chauvin, A., Pascaud, F., Kellenberger, S., and Farmer, E.E. (2013). Glutamate receptor-like genes mediate leaf-to-leaf wound signalling. Nature *500*, 422–426. https://doi.org/10.1038/nature12478.
14. Toyota, M., Spencer, D., Sawai-Toyota, S., Jiaqi, W., Zhang, T., Koo, A.J., Howe, G.A., and Gilroy, S. (2018). Glutamate triggers long-distance, calcium-based plant defense signaling. Science *361*, 1112–1115. https://doi.org/10.1126/science.aat7744.
15. Pearce, G., Strydom, D., Johnson, S., and Ryan, C.A. (1991). A polypeptide from tomato leaves induces wound-inducible proteinase inhibitor proteins. Science *253*, 895–897. https://doi.org/10.1126/science.253.5022.895.
16. Farmer, E.E., and Ryan, C.A. (1990). Interplant communication: airborne methyl jasmonate induces synthesis of proteinase inhibitors in plant leaves. Proc. Natl. Acad. Sci. USA *87*, 7713–7716. https://doi.org/10.1073/pnas.87.19.7713.
17. Hander, T., Fernández-Fernández, Á.D., Kumpf, R.P., Willems, P., Schatowitz, H., Rombaut, D., Staes, A., Nolf, J., Pottie, R., Yao, P.F., et al. (2019). Damage on plants activates Ca^{2+}-dependent metacaspases for release of immunomodulatory peptides. Science *363*, eaar7486. https://doi.org/10.1126/science.aar7486.
18. McGurl, B., Pearce, G., Orozco-Cardenas, M., and Ryan, C.A. (1992). Structure, expression, and antisense inhibition of the systemin precursor gene. Science *255*, 1570–1573. https://doi.org/10.1126/science.1549783.
19. El Oirdi, M., El Rahman, T.A., Rigano, L., El Hadrami, A., Rodriguez, M.C., Daayf, F., Vojnov, A., and Bouarab, K. (2011). Manipulates the antagonistic effects between immune pathways to promote disease development in tomato. Plant Cell *23*, 2405–2421. https://doi.org/10.1105/tpc.111.083394.
20. McGurl, B., Orozco-Cardenas, M., Pearce, G., and Ryan, C.A. (1994). Overexpression of the prosystemin gene in transgenic tomato plants generates a systemic signal that constitutively induces proteinase inhibitor synthesis. Proc. Natl. Acad. Sci. USA *91*, 9799–9802. https://doi.org/10.1073/pnas.91.21.9799.
21. Yan, L., Zhai, Q., Wei, J., Li, S., Wang, B., Huang, T., Du, M., Sun, J., Kang, L., Li, C.B., et al. (2013). Role of tomato lipoxygenase D in wound-induced jasmonate biosynthesis and plant immunity to insect herbivores. PLoS Genet. *9*, e1003964. https://doi.org/10.1371/journal.pgen.1003964.
22. Li, C., Liu, G., Xu, C., Lee, G.I., Bauer, P., Ling, H.Q., Ganal, M.W., and Howe, G.A. (2003). The tomato *suppressor of prosystemin-mediated responses2* gene encodes a fatty acid desaturase required for the biosynthesis of jasmonic acid and the production of a systemic wound signal for defense gene expression. Plant Cell *15*, 1646–1661. https://doi.org/10.1105/tpc.012237.
23. Schilmiller, A.L., and Howe, G.A. (2005). Systemic signaling in the wound response. Curr. Opin. Plant Biol. *8*, 369–377. https://doi.org/10.1016/j.pbi.2005.05.008.
24. Huffaker, A. (2015). Plant elicitor peptides in induced defense against insects. Curr. Opin. Insect Sci. *9*, 44–50. https://doi.org/10.1016/j.cois.2015.06.003.

25. Li, L., Li, C., Lee, G.I., and Howe, G.A. (2002). Distinct roles for jasmonate synthesis and action in the systemic wound response of tomato. Proc. Natl. Acad. Sci. USA *99*, 6416–6421. https://doi.org/10.1073/pnas.072072599.

26. Ryan, C.A., and Moura, D.S. (2002). Systemic wound signaling in plants: a new perception. Proc. Natl. Acad. Sci. USA *99*, 6519–6520. https://doi.org/10.1073/pnas.112196499.

27. Lee, G.I., and Howe, G.A. (2003). The tomato mutant spr1 is defective in systemin perception and the production of a systemic wound signal for defense gene expression. Plant J. *33*, 567–576. https://doi.org/10.1046/j.1365-313x.2003.01646.x.

28. Gust, A.A., Pruitt, R., and Nürnberger, T. (2017). Sensing danger: key to activating plant immunity. Trends Plant Sci. *22*, 779–791. https://doi.org/10.1016/j.tplants.2017.07.005.

29. De Lorenzo, G., Ferrari, S., Cervone, F., and Okun, E. (2018). Extracellular DAMPs in plants and mammals: immunity, tissue damage and repair. Trends Immunol. *39*, 937–950. https://doi.org/10.1016/j.it.2018.09.006.

30. Huber-Lang, M., Lambris, J.D., and Ward, P.A. (2018). Innate immune responses to trauma. Nat. Immunol. *19*, 327–341. https://doi.org/10.1038/s41590-018-0064-8.

31. Nürnberger, T., Brunner, F., Kemmerling, B., and Piater, L. (2004). Innate immunity in plants and animals: striking similarities and obvious differences. Immunol. Rev. *198*, 249–266. https://doi.org/10.1111/j.0105-2896.2004.0119.x.

32. Hou, S., Liu, D., and He, P. (2021). Phytocytokines function as immunological modulators of plant immunity. Stress Biol. *1*, 8. https://doi.org/10.1007/s44154-021-00009-y.

33. Liu, Z., Hou, S., Rodrigues, O., Wang, P., Luo, D., Munemasa, S., Lei, J., Liu, J., Ortiz-Morea, F.A., Wang, X., et al. (2022). Phytocytokine signalling reopens stomata in plant immunity and water loss. Nature *605*, 332–339. https://doi.org/10.1038/s41586-022-04684-3.

34. Tanaka, K., and Heil, M. (2021). Damage-associated molecular patterns (DAMPs) in plant innate immunity: applying the danger model and evolutionary perspectives. Annu. Rev. Phytopathol. *59*, 53–75. https://doi.org/10.1146/annurev-phyto-082718-100146.

35. Beloshistov, R.E., Dreizler, K., Galiullina, R.A., Tuzhikov, A.I., Serebryakova, M.V., Reichardt, S., Shaw, J., Taliansky, M.E., Pfannstiel, J., Chichkova, N.V., et al. (2018). Phytaspase-mediated precursor processing and maturation of the wound hormone systemin. New Phytol. *218*, 1167–1178. https://doi.org/10.1111/nph.14568.

36. Du, M., Zhao, J., Tzeng, D.T.W., Liu, Y., Deng, L., Yang, T., Zhai, Q., Wu, F., Huang, Z., Zhou, M., et al. (2017). MYC2 orchestrates a hierarchical transcriptional cascade that regulates jasmonate-mediated plant immunity in tomato. Plant Cell *29*, 1883–1906. https://doi.org/10.1105/tpc.16.00953.

37. Boter, M., Ruíz-Rivero, O., Abdeen, A., and Prat, S. (2004). Conserved MYC transcription factors play a key role in jasmonate signaling both in tomato and Arabidopsis. Genes Dev. *18*, 1577–1591. https://doi.org/10.1101/gad.297704.

38. Lorenzo, O., Chico, J.M., Sánchez-Serrano, J.J., and Solano, R. (2004). Jasmonate-insensitive1 encodes a MYC transcription factor essential to discriminate between different jasmonate-regulated defense responses in Arabidopsis. Plant Cell *16*, 1938–1950. https://doi.org/10.1105/tpc.022319.

39. Wang, L., Einig, E., Almeida-Trapp, M., Albert, M., Fliegmann, J., Mithöfer, A., Kalbacher, H., and Felix, G. (2018). The systemin receptor SYR1 enhances resistance of tomato against herbivorous insects. Nat. Plants *4*, 152–156. https://doi.org/10.1038/s41477-018-0106-0.

40. Couto, D., and Zipfel, C. (2016). Regulation of pattern recognition receptor signalling in plants. Nat. Rev. Immunol. *16*, 537–552. https://doi.org/10.1038/nri.2016.77.

41. Zhai, Q., Deng, L., and Li, C. (2020). Mediator subunit MED25: at the nexus of jasmonate signaling. Curr. Opin. Plant Biol. *57*, 78–86. https://doi.org/10.1016/j.pbi.2020.06.006.

42. Peng, H.C., and Kaloshian, I. (2014). The tomato leucine-rich repeat receptor-like kinases SlSERK3A and SlSERK3B have overlapping functions in bacterial and nematode innate immunity. PLoS One *9*, e93302. https://doi.org/10.1371/journal.pone.0093302.

43. Ma, X., Xu, G., He, P., and Shan, L. (2016). Serking coreceptors for receptors. Trends Plant Sci. *21*, 1017–1033. https://doi.org/10.1016/j.tplants.2016.08.014.

44. Fontes, E.P.B. (2024). SERKs and NIKs: coreceptors or signaling hubs in a complex crosstalk between growth and defense? Curr. Opin. Plant Biol. *77*, 102447. https://doi.org/10.1016/j.pbi.2023.102447.

45. Dean, R., Van Kan, J.A.L., Pretorius, Z.A., Hammond-Kosack, K.E., Di Pietro, A., Spanu, P.D., Rudd, J.J., Dickman, M., Kahmann, R., Ellis, J., et al. (2012). The Top 10 fungal pathogens in molecular plant pathology. Mol. Plant Pathol. *13*, 414–430. https://doi.org/10.1111/j.1364-3703.2011.00783.x.

46. Meindl, T., Boller, T., and Felix, G. (1998). The plant wound hormone systemin binds with the N-terminal part to its receptor but needs the C-terminal part to activate it. Plant Cell *10*, 1561–1570. https://doi.org/10.1105/tpc.10.9.1561.

47. Yoo, S.D., Cho, Y.H., and Sheen, J. (2007). Arabidopsis mesophyll protoplasts: a versatile cell system for transient gene expression analysis. Nat. Protoc. *2*, 1565–1572. https://doi.org/10.1038/nprot.2007.199.

48. Li, J., Wen, J., Lease, K.A., Doke, J.T., Tax, F.E., and Walker, J.C. (2002). BAK1, an Arabidopsis LRR receptor-like protein kinase, interacts with BRI1 and modulates brassinosteroid signaling. Cell *110*, 213–222. https://doi.org/10.1016/s0092-8674(02)00812-7.

49. Kandoth, P.K., Ranf, S., Pancholi, S.S., Jayanty, S., Walla, M.D., Miller, W., Howe, G.A., Lincoln, D.E., and Stratmann, J.W. (2007). Tomato MAPKs LeMPK1, LeMPK2, and LeMPK3 function in the systemin-mediated defense response against herbivorous insects. Proc. Natl. Acad. Sci. USA *104*, 12205–12210. https://doi.org/10.1073/pnas.0700344104.

50. Zuo, J., Niu, Q.W., and Chua, N.H. (2000). Technical advance: an estrogen receptor-based transactivator XVE mediates highly inducible gene expression in transgenic plants. Plant J. *24*, 265–273. https://doi.org/10.1046/j.1365-313x.2000.00868.x.

51. Liu, Y.Y., Du, M.M., Deng, L., Shen, J.F., Fang, M.M., Chen, Q., Lu, Y.H., Wang, Q.M., Li, C.Y., and Zhai, Q.Z. (2019). MYC2 regulates the termination of jasmonate signaling via an autoregulatory negative feedback loop. Plant Cell *31*, 106–127. https://doi.org/10.1105/tpc.18.00405.

52. Lee, J.S., Hnilova, M., Maes, M., Lin, Y.C.L., Putarjunan, A., Han, S.K., Avila, J., and Torii, K.U. (2015). Competitive binding of antagonistic peptides fine-tunes stomatal patterning. Nature *522*, 439–443. https://doi.org/10.1038/nature14561.

53. Lan, Z., Song, Z., Wang, Z., Li, L., Liu, Y., Zhi, S., Wang, R., Wang, J., Li, Q., Bleckmann, A., et al. (2023). Antagonistic RALF peptides control an intergeneric hybridization barrier on Brassicaceae stigmas. Cell *186*, 4773–4787.e12. https://doi.org/10.1016/j.cell.2023.09.003.

54. Bortolotti, P., Faure, E., and Kipnis, E. (2018). Inflammasomes in tissue damages and immune disorders after trauma. Front. Immunol. *9*, 1900. https://doi.org/10.3389/fimmu.2018.01900.

55. Zhou, W., Lozano-Torres, J.L., Blilou, I., Zhang, X., Zhai, Q., Smant, G., Li, C., and Scheres, B. (2019). A jasmonate signaling network activates root stem cells and promotes regeneration. Cell *177*, 942–956.e14. https://doi.org/10.1016/j.cell.2019.03.006.

56. Yang, W., Zhai, H., Wu, F., Deng, L., Chao, Y., Meng, X., Chen, Q., Liu, C., Bie, X., Sun, C., et al. (2024). Peptide REF1 is a local wound signal promoting plant regeneration. Cell *187*, 3024–3038.e14. https://doi.org/10.1016/j.cell.2024.04.040.

57. Sun, J.Q., Jiang, H.L., and Li, C.Y. (2011). Systemin/jasmonate-mediated systemic defense signaling in tomato. Mol. Plant *4*, 607–615. https://doi.org/10.1093/mp/ssr008.

58. He, Z., Webster, S., and He, S.Y. (2022). Growth-defense trade-offs in plants. Curr. Biol. *32*, R634–R639. https://doi.org/10.1016/j.cub.2022.04.070.

59. Karasov, T.L., Chae, E., Herman, J.J., and Bergelson, J. (2017). Mechanisms to mitigate the trade-off between growth and defense. Plant Cell *29*, 666–680. https://doi.org/10.1105/tpc.16.00931.

60. Schneider, C.A., Rasband, W.S., and Eliceiri, K.W. (2012). NIH Image to ImageJ: 25 years of image analysis. Nat. Methods *9*, 671–675. https://doi.org/10.1038/nmeth.2089.

61. Li, H., Handsaker, B., Wysoker, A., Fennell, T., Ruan, J., Homer, N., Marth, G., Abecasis, G., and Durbin, R.; 1000 Genome Project Data Processing Subgroup (2009). The Sequence Alignment/Map format and SAMtools. Bioinformatics *25*, 2078–2079. https://doi.org/10.1093/bioinformatics/btp352.

62. Abe, A., Kosugi, S., Yoshida, K., Natsume, S., Takagi, H., Kanzaki, H., Matsumura, H., Yoshida, K., Mitsuoka, C., Tamiru, M., et al. (2012). Genome sequencing reveals agronomically important loci in rice using MutMap. Nat. Biotechnol. *30*, 174–178. https://doi.org/10.1038/nbt.2095.

63. Danecek, P., Auton, A., Abecasis, G., Albers, C.A., Banks, E., DePristo, M.A., Handsaker, R.E., Lunter, G., Marth, G.T., Sherry, S.T., et al. (2011). The variant call format and VCFtools. Bioinformatics *27*, 2156–2158. https://doi.org/10.1093/bioinformatics/btr330.

64. Liu, Z., Jia, Y., Ding, Y., Shi, Y., Li, Z., Guo, Y., Gong, Z., and Yang, S. (2017). Plasma membrane CRPK1-mediated phosphorylation of 14–3-3 proteins induces their nuclear import to fine-tune CBF signaling during cold response. Mol. Cell *66*, 117–128.e5. https://doi.org/10.1016/j.molcel.2017.02.016.

65. Li, X., Lin, H., Zhang, W., Zou, Y., Zhang, J., Tang, X., and Zhou, J.M. (2005). Flagellin induces innate immunity in nonhost interactions that is suppressed by Pseudomonas syringae effectors. Proc. Natl. Acad. Sci. USA *102*, 12990–12995. https://doi.org/10.1073/pnas.0502425102.

66. You, Y., Zhai, Q., An, C., and Li, C. (2019). LEUNIG_HOMOLOG mediates MYC2-dependent transcriptional activation in cooperation with the coactivators HAC1 and MED25. Plant Cell *31*, 2187–2205. https://doi.org/10.1105/tpc.19.00115.

67. Deng, L., Wang, H., Sun, C.L., Li, Q., Jiang, H.L., Du, M.M., Li, C.B., and Li, C.Y. (2018). Efficient generation of pink-fruited tomatoes using CRISPR/Cas9 system. J. Genet. Genomics *45*, 51–54. https://doi.org/10.1016/j.jgg.2017.10.002.

68. Li, L., Zhao, Y.F., McCaig, B.C., Wingerd, B.A., Wang, J.H., Whalon, M.E., Pichersky, E., and Howe, G.A. (2004). The tomato homolog of CORONATINE-INSENSITIVE1 is required for the maternal control of seed maturation, jasmonate-signaled defense responses, and glandular trichome development. Plant Cell *16*, 126–143. https://doi.org/10.1105/tpc.017954.

69. You, Y., An, C., and Li, C. (2020). Insect feeding assays with *Spodoptera exigua* on *Arabidopsis thaliana*. Bio Protoc. *10*, e3538. https://doi.org/10.21769/BioProtoc.3538.

70. Lian, J., Han, H., Zhao, J., and Li, C. (2018). In-vitro and in-planta *Botrytis cinerea* inoculation assays for tomato. Bio Protoc. *8*, e2810. https://doi.org/10.21769/BioProtoc.2810.

71. Li, H., and Durbin, R. (2009). Fast and accurate short read alignment with Burrows-Wheeler transform. Bioinformatics *25*, 1754–1760. https://doi.org/10.1093/bioinformatics/btp324.

72. Li, H. (2013). Aligning sequence reads, clone sequences and assembly contigs with BWA-MEM. Preprint at arXiv. https://doi.org/10.48550/arXiv.1303.3997.

73. Takagi, H., Abe, A., Yoshida, K., Kosugi, S., Natsume, S., Mitsuoka, C., Uemura, A., Utsushi, H., Tamiru, M., Takuno, S., et al. (2013). QTL-seq: rapid mapping of quantitative trait loci in rice by whole genome resequencing of DNA from two bulked populations. Plant J. *74*, 174–183. https://doi.org/10.1111/tpj.12105.

74. Ge, Z., Bergonci, T., Zhao, Y., Zou, Y., Du, S., Liu, M.C., Luo, X., Ruan, H., García-Valencia, L.E., Zhong, S., et al. (2017). Arabidopsis pollen tube integrity and sperm release are regulated by RALF-mediated signaling. Science *358*, 1596–1600. https://doi.org/10.1126/science.aao3642.

75. Stegmann, M., Monaghan, J., Smakowska-Luzan, E., Rovenich, H., Lehner, A., Holton, N., Belkhadir, Y., and Zipfel, C. (2017). The receptor kinase FER is a RALF-regulated scaffold controlling plant immune signaling. Science *355*, 287–289. https://doi.org/10.1126/science.aal2541.

76. Butenko, M.A., Wildhagen, M., Albert, M., Jehle, A., Kalbacher, H., Aalen, R.B., and Felix, G. (2014). Tools and strategies to match peptide-ligand receptor pairs. Plant Cell *26*, 1838–1847. https://doi.org/10.1105/tpc.113.120071.

77. Wang, L., Albert, M., Einig, E., Fürst, U., Krust, D., and Felix, G. (2016). The pattern-recognition receptor CORE of Solanaceae detects bacterial cold-shock protein. Nat. Plants *2*, 16185. https://doi.org/10.1038/nplants.2016.185.

78. Sainsbury, F., Thuenemann, E.C., and Lomonossoff, G.P. (2009). pEAQ: versatile expression vectors for easy and quick transient expression of heterologous proteins in plants. Plant Biotechnol. J. *7*, 682–693. https://doi.org/10.1111/j.1467-7652.2009.00434.x.

79. Xiao, Y., Stegmann, M., Han, Z., DeFalco, T.A., Parys, K., Xu, L., Belkhadir, Y., Zipfel, C., and Chai, J. (2019). Mechanisms of RALF peptide perception by a heterotypic receptor complex. Nature *572*, 270–274. https://doi.org/10.1038/s41586-019-1409-7.

80. Sun, Y., Li, L., Macho, A.P., Han, Z., Hu, Z., Zipfel, C., Zhou, J.M., and Chai, J. (2013). Structural basis for flg22-induced activation of the Arabidopsis FLS2-BAK1 immune complex. Science *342*, 624–628. https://doi.org/10.1126/science.1243825.

81. Macho, A.P., Schwessinger, B., Ntoukakis, V., Brutus, A., Segonzac, C., Roy, S., Kadota, Y., Oh, M.H., Sklenar, J., Derbyshire, P., et al. (2014). A bacterial tyrosine phosphatase inhibits plant pattern recognition receptor activation. Science *343*, 1509–1512. https://doi.org/10.1126/science.1248849.

82. Zhang, J., Shao, F., Li, Y., Cui, H., Chen, L., Li, H., Zou, Y., Long, C., Lan, L., Chai, J., et al. (2007). A *Pseudomonas syringae* effector inactivates MAPKs to suppress PAMP-Induced immunity in plants. Cell Host Microbe *1*, 175–185. https://doi.org/10.1016/j.chom.2007.03.006.

Please cite this article in press as: Zhou et al., Antagonistic systemin receptors integrate the activation and attenuation of systemic wound signaling in tomato, Developmental Cell (2024), https://doi.org/10.1016/j.devcel.2024.11.005

STAR★METHODS

KEY RESOURCES TABLE

REAGENT or RESOURCE	SOURCE	IDENTIFIER
Antibodies		
Mouse monoclonal anti-GFP for western blot	YTHXBio	Cat#ZA009
Mouse monoclonal anti-myc	Abmart	Cat#M20002L; RRID: AB_2861172
Mouse monoclonal anti-Flag	Abmart	Cat#M20008L; RRID: AB_2713960
Rabbit monoclonal anti-pERK	Cell Signaling	Cat#4370; RRID: AB_2315112
Rabbit polyclonal anti-GFP for ChIP	Abcam	Cat#AB290; RRID: AB_303395
Rabbit polyclonal anti-BiP	Agrisera	Cat#AS09481; RRID: AB_1832007
Rabbit polyclonal anti-AHA1	Agrisera	Cat#AS07260; RRID: AB_1031584
Rabbit polyclonal anti-RbcL	Agrisera	Cat#AS03037; RRID: AB_2175406
Goat Anti-Mouse IgG, HRP Conjugated	CWBIO	Cat#CW0102S; RRID: AB_2814710
Goat Anti-Rabbit IgG, HRP Conjugated	CWBIO	Cat#CW0103S; RRID: AB_2814709
Rabbit polyclonal anti-PRS	This paper	N/A
Mouse polyclonal anti-SERK3a	This paper	N/A
Bacterial and virus strains		
Agrobacterium tumefaciens GV3101	N/A	N/A
Escherichia coli BL21(DE3) pLysS	TIANGEN	Cat#CB106-02
Escherichia coli TOP10	Biomed	BC101-01
Chemicals, peptides, and recombinant proteins		
Dynabeads™ Protein G	Invitrogen	Cat#10004D
Myc-Trap Agarose beads	Proteintech	Cat# yta-20
Anti-FLAG® M2 agarose beads (affinity gel) for Co-IP	Sigma-Aldrich	Cat#A2220
anti-FLAG affinity resin for IP	Genscript	Cat#L00766
GST Bind Resin	Merck Millipore	Cat#70541-4
Ni-NTA His•Bind® Resin	Novagen	Cat#70666
amylase resin	New England Biolabs	Cat#E8021L
Protease Inhibitor Cocktail	Roche	Cat#05056489001
Streptavidin Magnetic Particles	Spherotech	Cat#SVMS-30-10
Acridinium NHS ester	GLPBIO	Cat#GC42711
Methyl jasmonate	Sigma-Aldrich	Cat#J2500
Acridinium-conjugated systemin peptide	Scilight Biotechnology	Custom order
flg22 peptide	Scilight Biotechnology	Custom order
systemin1-14 peptide	Scilight Biotechnology	Custom order
systemin peptide	Scilight Biotechnology	Custom order
Biotinylated systemin peptide	Scilight Biotechnology	Custom order
L-012	Wako	Cat#120-04891
Peroxidase	Sigma-Aldrich	Cat#P6782
β-estradiol	Sigma-Aldrich	Cat# E8875

(*Continued on next page*)

Please cite this article in press as: Zhou et al., Antagonistic systemin receptors integrate the activation and attenuation of systemic wound signaling in tomato, Developmental Cell (2024), https://doi.org/10.1016/j.devcel.2024.11.005

Continued

REAGENT or RESOURCE	SOURCE	IDENTIFIER
TRIzol	Invitrogen	Cat#15596018
Critical commercial assays		
Dual-Luciferase Reporter Assay System	Promega	Cat#E1960
ClonExpress II one Step Cloning Kit	Vazyme	Cat#C115
QIAquick PCR Purification Kit	QIAGEN	Cat#28106
PrimeScript RT kit	Takara	Cat#RR0447A
KAPA SYBR Fast qPCR kit	KAPA Biosystems	Cat#KK4601
Monolith™ Protein Labeling Kit	NanoTemper	Cat#MO-L001
Monolith™ Standard Treated Capillaries	NanoTemper	Cat#MO-K022
Minute Plant Plasma Membrane Protein Isolation Kit	Invent Biotechnologies	Cat#SM-005-P
Chemiluminescent EMSA kit	Beyotime	Cat#GS009
Deposited data		
Raw and analyzed data from bulk population sequencing	This paper	GSA: CRA004447
Experimental models: Organisms/strains		
Solanum lycopersicum cv. Castlemart (CM; LA2400)	N/A	N/A
Solanum lycopersicum cv. Ailsa Craig (AC; LA2838A)	N/A	N/A
Solanum lycopersicum: *spr1-1*	Lee and Howe[27]	N/A
Solanum lycopersicum: *spr1-2*	Lee and Howe[27]	N/A
Solanum lycopersicum: *35S::PRS*	Li et al.[22]	N/A
Solanum lycopersicum: *syr1*	This paper	N/A
Solanum lycopersicum: *syr2*	This paper	N/A
Solanum lycopersicum: *syr1 syr2*	This paper	N/A
Solanum lycopersicum: *serk3a*	This paper	N/A
Solanum lycopersicum: *serk3b*	This paper	N/A
Solanum lycopersicum: *ProSYR1::SYR1/spr1-1* (*Comp*)	This paper	N/A
Solanum lycopersicum: *35S::SYR1-HA-FLAG* (*SYR1-OE*)	This paper	N/A
Solanum lycopersicum: *35S::SYR2-HA-FLAG* (*SYR2-OE*)	This paper	N/A
Solanum lycopersicum: *35S::SYR2-HA-FLAG/syr1-1* (*SYR2-OE/syr1-1*)	This paper	N/A
Solanum lycopersicum: *MYC2-RNAi*	Yan et al.[21]	N/A
Solanum lycopersicum: *MYC2-GFP*	Du et al.[36]	N/A
Nicotiana benthamiana	N/A	N/A
Arabidopsis thaliana Col-0	ABRC	CS2004
Oligonucleotides		
Primers used in this study, see Table S1	This paper	N/A
Recombinant DNA		
pTX041-SYR1	This paper	N/A
pTX041-SYR2	This paper	N/A
pTX041-SERK3a	This paper	N/A
pTX041-SERK3b	This paper	N/A
pCAMBIA1300-pSYR1-SYR1	This paper	N/A
pCM1307-35S-SYR1-HA-FLAG	This paper	N/A
pCM1307-35S-SYR2-HA-FLAG	This paper	N/A
pCM1307-35S-SYR1^{Ecto}-HA-FLAG	This paper	N/A

(*Continued on next page*)

Please cite this article in press as: Zhou et al., Antagonistic systemin receptors integrate the activation and attenuation of systemic wound signaling in tomato, Developmental Cell (2024), https://doi.org/10.1016/j.devcel.2024.11.005

Continued

REAGENT or RESOURCE	SOURCE	IDENTIFIER
pCM1307-35S-SYR2^{Ecto}-HA-FLAG	This paper	N/A
pGWB17-35S-SERK3a-myc	This paper	N/A
pEAQ-35S-SYR1^{Ecto}-Flag-His	This paper	N/A
pEAQ-35S-SYR2^{Ecto}-Flag-His	This paper	N/A
pK7FWG2.0-35S-SYR1-GFP	This paper	N/A
pK7FWG2.0-35S-SYR2-GFP	This paper	N/A
pER8-SYR2-GFP	This paper	N/A
pMAL-c2X-MYC2	Liu et al.[51]	N/A
pFastBac1-SERK3a^{Ecto}	This paper	N/A
pGEX-4T-3-GST-SYR1^{CD}	This paper	N/A
pGEX-4T-3-GST-SYR1$^{Y952N-CD}$	This paper	N/A
pGEX-4T-3-GST-SYR2^{CD}	This paper	N/A
pUC19-35S-SYR1-FLAG	This paper	N/A
pUC19-35S-SYR2-FLAG	This paper	N/A
Software and algorithms		
ImageJ	Schneider et al.[60]	https://imagej.nih.gov/ij/
R (v3.5.3)	N/A	N/A
Prism 8	GraphPad	https://www.graphpad.com/
BWA-MEM 0.7.15	–	http://bio-bwa.sourceforge.net/
PicardTools 2.0.1	–	https://broadinstitute.github.io/picard/
Samtools 1.9	Li et al.[61]	http://samtools.sourceforge.net/
bcftools 1.9	–	https://samtools.github.io/bcftools/bcftools.html
MutMap	Abe et al.[62]	https://doi.org/10.1038/nbt.2095.
VCFtools 0.1.17	Danecek et al.[63]	https://vcftools.github.io/man_latest.html

EXPERIMENTAL MODEL AND STUDY PARTICIPANT DETAILS

Plant material and growth conditions

Seeds of *Solanum lycopersicum* cv. Ailsa Craig (AC; LA2838A) and cv. Castlemart (CM; LA2400) were obtained from TGRC (Tomato Genetics Resource Center; https://tgrc.ucdavis.edu). AC was used as the wild type (WT) for most plant materials. For *spr1-1* and *spr1-2*, CM was used as the WT. The following tomato genotypes were used in this study: *spr1-1* and *spr1-2*,[27] *syr1*, *syr2*, *syr1 syr2*, *serk3a*, *serk3b*, *35S::PRS*,[22] *MYC2-RNAi*,[21] *MYC2-GFP*,[36] *ProSYR1::SYR1/spr1-1* (*Comp*), *SYR1-OE* (*35S::SYR1-HA-Flag*/AC), *SYR2-OE* (*35S::SYR2-HA-Flag*/AC) and *SYR2-OE/syr1-1* (*35S::SYR2-HA-Flag/syr1-1*). Seeds of *N. benthamiana* are from our own stocks.

Tomato seeds were germinated on moistened filter paper at room temperature and then sown in 32-cell plastic flats. Seedlings were grown in growth chamber and maintained at 60% relative humidity under 16 h of light (200 μE m^{-2} s^{-1}) at 26°C and 8 h of dark at 18°C. *N. benthamiana* seeds were directly sown in soil in 8 cm diameter pots and grown under the same conditions for 10 d before being transplanted to the 32-cell plastic flats.

Biomass and phenotypic analyses of CM, *spr1-1*, *spr1-2*, AC, *syr1-1*, *syr1-2*, *syr2-1* and *syr2-2* were conducted on plants grown in the experimental field at the Institute of Genetics and Developmental Biology (IGDB) in Beijing in the natural growing season. Germinating seeds were sown in 50-cell flats and grown in growth chamber for 30 d before being transplanted to the field. Plants were grown under standard water and fertilizer management.

METHOD DETAILS

Plasmid construction and plant transformation

To generate ectodomain constructs for *in vitro* pull-down assays, DNA fragments of the *SYR1* coding sequence (CDS) (1-2340 bp) and *SYR2* CDS (1-2325 bp) were cloned into the pCM1307 (HA-Flag tag) vector[64] using a ClonExpress II one Step Cloning Kit (Vazyme Biotech cat#C115) to generate *SYR1^{Ecto}-HA-Flag* and *SYR2^{Ecto}-HA-Flag* constructs, respectively.

To generate constructs for recombinant proteins for *in vitro* phosphorylation assays, $SYR1^{CD}$ (2410-3348 bp), $SYR2^{CD}$ (2395-3348 bp) were cloned into the pGEX-4T-3 vector to create translational fusion to GST tag. Point mutations were introduced into the above constructs by site-directed mutagenesis.

To generate constructs for transient expression assay in protoplasts, *SYR1* CDS, *SYR2* CDS were cloned into the pUC19-35S-Flag-RBS vector[65] using a ClonExpress II one Step Cloning Kit (Vazyme Biotech cat#C115).

To generate constructs for *N. benthamiana* transient expression assays, *SYR1* CDS and *SYR2* CDS were cloned into the pK7FWG2.0 (GFP tag) or pCM1307 (HA-Flag tag) vectors. *SERK3a* CDS was cloned into the pGWB17 (myc tag) vector. For the β-estradiol-inducible *SYR2-GFP* construct, *SYR2* CDS was fused with GFP tag and cloned into the pER8 vector.[50]

For genetic complementation of the *spr1-1* mutant, a *SYR1* genomic fragment containing its 2016-bp promoter sequence and coding sequence was cloned into the pCAMBIA1300 vector[66] to generate the *ProSYR1::SYR1* construct. *SYR1* CDS and *SYR2* CDS were cloned into the pCM1307 vector[64] to generate the *Pro35S::SYR1-HA-Flag* and *Pro35S::SYR2-HA-Flag* constructs. All constructs were introduced into tomato via *Agrobacterium tumefaciens*-mediated transformation. Transformants were selected based on their resistance to hygromycin B or kanamycin. Homozygous T2 or T3 transgenic plants were used for further experiments. All primers used for plasmid construction and genotyping are listed in Table S1.

CRISPR-Cas9-mediated mutation

Null mutations of *SYR1*, *SYR2*, *SERK3a* and *SERK3b* were generated by the tomatoU6 promoter-controlled CRISPR-Cas9 system as previously described.[67] Briefly, two sets of primers containing guide RNA (gRNA) sequences of *SYR1* were used in PCR to generate a tomato *U6-26-SYR1-gRNA* cassette. The resulting *U6-26-SYR1-gRNA* cassette was then cloned into the binary vector pCBC-DT1T2_tomatoU6 to form the *SYR1-pTX041* construct. The *SYR2-pTX041*, *SERK3a-pTX041* and *SERK3b-pTX041* constructs were generated following the same protocol. The final binary vectors were transformed into tomato via *Agrobacterium*-mediated transformation. CRISPR-Cas9-mediated mutations were genotyped by PCR amplification and DNA sequencing. *syr1 syr2* double mutant lines were generated by transforming the *SYR2-pTX041* construct into *syr1-1* mutant. Homozygous lines without Cas9 were identified for further experiments. Primers used for plasmid construction and genotyping are listed in Table S1.

Wounding, systemin and MeJA treatment of tomato seedlings

For wounding treatment, 18-d-old (with two expanded leaves and a third emerging leaf) seedlings were wounded once with a hemostat across the midrib of all leaflets on the lower (older) leaves as described.[22] Wounded plants were incubated under continuous illumination. After 12 h, lower damaged (local response) and upper undamaged (systemic response) leaves were harvested for RNA extraction and gene expression assays. Leaves of unwound plants were harvested as control. Leaf tissues of five plants were pooled for each sample.

Systemin treatment was performed as described with modification.[22] Eighteen-d-old tomato seedlings were excised at the base of the stem and placed in 0.5 mL microfuge tubes containing 400 μL 100 nM systemin. After 2 h, plants were transferred to 1.5 mL microfuge tubes containing 1.5 mL of water, and incubated in a lucite box under continuous illumination. Twelve hours later, leaf tissues of five plants were pooled for RNA extraction and RT-qPCR assays. Control plants were fed with water.

MeJA treatment was performed as described previously,[68] 18-d-old seedlings were enclosed in a lucite box (10×32×60 cm) containing 5 μL of MeJA applied to cotton wicks that were spaced evenly within the box. Plants exposed to MeJA vapor were harvested after 12 h and used for RNA extraction and RT-qPCR assays.

flg22 peptide (QRLSTGSRINSAKDDAAGLQIA), systemin peptide (AVQSKPP SKRDPPKMQTD), $systemin^{1-14}$ (AVQSKPPSKRDPPK), acri-systemin (AVQSKPP SKRDPPK-acridinium-MQTD) and Biotin-systemin (AVQSKPPSKRDPPK-Biotin-MQTD) were commercially synthesized by Scilight Biotechnology, China. Acridinium esters and biotins were conjugated to the lysine, the 14th amino acid of systemin. Acridinium NHS ester was purchased from GLPBIO (cat#GC42711). MeJA was purchased from Sigma-Aldrich (cat#J2500).

Root growth inhibition and biomass reduction assays

For systemin-induced root growth inhibition or peptide-induced biomass reduction assays, seeds were sterilized and then plated on one half-strength Murashige and Skoog medium (Phytotech, cat#M519) containing 1% (w/v) sucrose. At radical emergence, seeds were transferred to plates containing the same medium as above with the addition of 100 nM systemin. The plates were then placed vertically and seedlings grown for 5 (root growth inhibition) or 6 d (biomass reduction), respectively. Seedlings were grown in growth chamber and maintained at 60% relative humidity under 16 h of light (200 $\mu E\ m^{-2}\ s^{-1}$) at 28°C and 8 h of dark at 18°C. The root length and biomass of at least 20 seedlings was measured for per treatment. Control plants were grown on medium without peptides.

Insect feeding trials

Insect feeding assays were performed as described with modifications.[69] Briefly, *Spodoptera exigua* eggs were hatched at 27°C. Third-instar *S. exigua* larvae were transferred to a Petri dish and starved for 12 h before being used in the feeding experiment. For each genotype, more than forty third-instar *S. exigua* larvae with similar weight were placed in 150 mm plastic Petri dishes with leaflets from 4-week-old plants. Leaves in each Petri dish were replaced every two days. Larvae weight was measured four days later.

To examine the effect of systemic wound responses on insect resistance, 4-week-old plants were wounded once with a hemostat across the midrib of all leaflets on the first compound leaf. After 12 h, all upper undamaged (systemic) leaves of wounded plants were collected for insect feeding trials. Leaves of the same position from unwounded plants were used as control.

Please cite this article in press as: Zhou et al., Antagonistic systemin receptors integrate the activation and attenuation of systemic wound signaling in tomato, Developmental Cell (2024), https://doi.org/10.1016/j.devcel.2024.11.005

Botrytis cinerea Inoculation Assays

Botrytis cinerea B05.10 inoculation assays were performed as described with modifications.[70] *B. cinerea* was cultured on 2×V8 agar (36% V8 juice, 0.2% $CaCO_3$, and 2% Bacto-agar) and incubated for 14 d at 24°C under a 12-h photoperiod before spore collection. Spore suspensions were prepared by collecting spores in 1% Sabouraud Maltose Broth (SMB), filtering through nylon mesh to remove hyphae, and adjusting the concentration to 10^6 spores/mL. Detached leaves from 4-week-old tomato plants were placed in Petri dishes containing 0.8% agar medium, with the petiole embedded in the medium for the pathogenicity test. Each leaflet was spotted with a single droplet of 3 μL *B. cinerea* spore suspension (10^6 spores/mL). The trays were covered with lids and kept under the same conditions until disease lesions were recorded 3 d later.

Measurement of endogenous systemin levels

Eighteen-d-old WT seedlings were wounded as described above. Leaves (1 g fresh weight) were extracted with 20% methanol (MeOH) containing 1% formic acid (FA) and [$^{13}C_5$, ^{15}N]-systemin (internal standard) overnight at 4 °C. The crude extracts were purified with WCX cartridge (Waters, USA). The peptide-containing fraction eluted with 2% trifluoroacetic acid in MeOH was collected, concentrated and reconstructed in 0.1% FA and subjected to ultra-high performance liquid chromatography-tandem mass spectrometry (UPLC-MS/MS) analysis using an Acquity UPLC System (Waters, USA) combined online with triple quadrupole linear ion trapping tandem mass spectrometer (QTRAP 6500; AB Sciex, USA) equipped with an ESI source. The separation of analytes was achieved on a Peptide CSH C18 column (100 mm × 2.1 mm, 1.7 μm). The UPLC method was as follows: mobile phase A: 0.1% FA in water, B: 0.1% FA in acetonitrile; gradient: 0-1 min, 1% B; 1-5 min, 1% B to 30% B; 5-8 min, 30% B to 100% B; 8-11 min, 100% B; 11-12.5 min, 100% B to 1% B; 12.5-14 min, 1% B. Systemin was detected in positive multiple reaction monitoring mode. The source parameters were set as: ionspray voltage, 5400 V; source temperature, 500 °C; nebulizer gas, 50 psi; desolvation gas, 50 psi; and curtain gas, 35 psi. Quantitation was performed using the isotope dilution method.

Bulk population sequencing

For bulk population sequencing, two DNA pools, *spr1*-type pool and WT-type pool, each with an equal amount of DNA from 100 F_2 individuals derived from a *spr1-1* × CM cross were prepared. Two pooled libraries and the two parent libraries were prepared with the Illumina TruSeq DNA PCR-free prep kit and sequenced using the Illumina HiSeq X-ten platform by Shanghai OE Biological Technology Co. Ltd. To identify the mutation site, reads were mapped to the tomato reference genome using BWA-MEM[71,72] with the default parameters. Alignments were then sorted with SAMtools and duplicates marked with Picard Tools.[61] SNPs were called with SAMtools/BCFtools.[61] In order to reduce false-positive detection of SNPs, SNP positions with a SNP quality score <20 and read depth <4 were filtered. The MutMap method with minor modifications was applied to detect mapping intervals associated with the phenotype as described previously.[62,73] Briefly, the ratio between the number of reads of a mutant SNP and the total number of reads covering the SNP site was defined as the SNP index. The ΔSNP index is defined by subtracting the SNP index value of WT-type pool from *spr1*-type pool. The average of ΔSNP index was calculated using a sliding-window approach with a 1-Mb window size (by 100-kb) and plotted across the 12 tomato chromosomes.

RNA extraction and gene expression analysis

Total RNA was extracted from each sample using a TRIzol kit (Invitrogen, cat#15596018) according to the manufacturer's instructions. The quality of the total RNA was determined using a NanoDrop spectrophotometer (Thermo Fisher). Each sample (2 μg) of total RNA was used to synthesize the first strand cDNA with the PrimeScript RT kit (Takara, cat#RR0447A). RT-qPCR was performed using a Roche LightCycler 480 system with the KAPA SYBR Fast qPCR kit (KAPA Biosystems, cat#KK4601). Expression levels of target genes were normalized against that of tomato *ACTIN2*. The gene expression levels were normalized to *ACTIN2*, and the expression levels in wild-type without treatment were arbitrarily set to 1. Error bars represent the SD from three independent experiments. Primers used to quantify gene expression levels are listed in Table S1.

Total protein extraction and immunoblot assays

Eighteen-d-old transgenic tomato seedlings or *N. benthamiana* leaves infiltrated with indicated constructs were ground into fine powders in liquid nitrogen and then transferred to extraction buffer (50 mM pH7.5 Tris-HCl, 150 mM NaCl, 0.1% [v/v] TritonX-100, 0.2% [v/v] NP-40,10 mM DTT) containing 1× protease inhibitor cocktail (Roche, cat#05056489001). For immunoblot analysis, protein samples were boiled for 5 min after mixing with SDS protein loading buffer, separated by SDS-PAGE, and then transferred to polyvinylidene fluoride membranes. Immunoblots were probed with anti-GFP antibody (YTHX, cat#ZA009), anti-myc antibody (Abmart, cat#M20002L), anti-Flag antibody (Abmart, cat#M20008L), anti-pERK antibody (Cell Signaling, cat#4370), Anti-H^+-ATPase 1 antibody (anti-AHA1, Agrisera, cat#AS07260), anti-Lumenal-binding protein antibody (anti-BiP; Agrisera, cat#AS09481) and anti-RubisCO large subunit antibody (anti-RbcL, Agrisera, cat#AS03037).

Subcellular fractionation assay

Eighteen-d-old seedlings of WT, *SYR1-HA-Flag* (*SYR1-OE-1*) and *SYR2-HA-Flag* (*SYR1-OE-1*) were wounded as described above. Leaves (~200 mg) were processed using Minute Plant Plasma Membrane Protein Isolation Kit (Invent Biotechnologies, cat#SM-005-P) according to the manufacturer's instructions. Each sample was separated into plasma membrane, organelle membrane and soluble fractions. Anti-AHA1, anti-BiP and anti-RbcL were used as marker for plasma membrane, organelle membrane and soluble

Please cite this article in press as: Zhou et al., Antagonistic systemin receptors integrate the activation and attenuation of systemic wound signaling in tomato, Developmental Cell (2024), https://doi.org/10.1016/j.devcel.2024.11.005

fractions, respectively. SYR1, SYR2 were detected with anti-Flag antibody, prosystemin and SERK3a were detected with their antibodies.

Antibody production

To generate prosystemin antibody, the synthesized peptide systemin was conjugated to a keyhole limpet haemocyanin carrier via SS-linkage through the N-terminal cysteine (KLH-C-AVQSKPPSKRDPPKMQTD), and polyclonal antisera were raised in rabbit (ABclonal). Prosystemin antibody was purified from the antisera by affinity chromatography using antigen-immobilized beads. The purified antibody was used for immunoblotting at a final concentration of 1:4,000. For generation of SERK3a antibody, the C-terminal of *SERK3a* (1636-1845 bp) was cloned into the pGEX-4T-3 vector. The recombinant GST-SERK3a$^{546\text{-}615}$ protein purified from *E. coli* was used to raise polyclonal antisera in mouse (Animal center, Institute of Genetics and Developmental Biology, Chinese Academy of Sciences), and the antisera was used for immunoblotting at a final concentration of 1:2,000.

Co-immunoprecipitation (co-IP) experiments

Co-IP experiments were performed as described previously with modifications.[66] Briefly, *A. tumefaciens* strains containing the desired constructs were infiltrated into fully expanded leaves of *N. benthamiana* plants. After incubation for 72 h, the infiltrated leaves were infiltrated with 100 nM systemin or H_2O for 30 min. Leaves were then lysed with protein extraction buffer (50 mM pH7.5 Tris-HCl, 150 mM NaCl, 0.1% [v/v] TritonX-100, 0.2% [v/v] NP-40, 10 mM DTT) containing 1× protease inhibitor cocktail (Roche, cat#05056489001). For anti-myc IP, protein extracts were incubated with 25 μL Myc-Trap Agarose beads (Proteintech, cat#yta-20) for 3 h, washed 6 times with extraction buffer, and then eluted by boiling the beads in SDS protein loading buffer for 5 min. Anti-Flag IP was performed in a similar manner, except that protein extracts were incubated with anti-Flag® M2 agarose beads (Sigma-Aldrich, cat#A2220). The eluted proteins were separated by SDS-PAGE and detected by immunoblot with corresponding antibodies.

The well-established XVE system[50] was employed to achieve chemical-inducible expression of SYR2-GFP. Briefly, *A. tumefaciens* strains containing the desired constructs were infiltrated into fully expanded leaves of *N. benthamiana* plants. After incubation for 48 h, the infiltrated leaves were further infiltrated with indicated concentrations of β-estradiol (Sigma-Aldrich, cat#E8875) and incubated for 24 h. The infiltrated leaves were then treated with systemin as described above before protein extraction and co-IP assays.

In vitro pull-down assays

Pull-down experiments between systemin peptide and Flag-tagged SYR1/2 ectodomains were conducted as described previously.[74,75] In more detail, 10 nM biotin-systemin and 1 ng/μL Flag-tagged proteins were mixed in 500 μL reaction buffer (50 mM Tris-HCl, pH 7.5, 1% IGEPAL) and kept at 4°C for 1 h. The samples mixed with 50 μL Streptavidin Magnetic Particles (Spherotech, cat#SVMS-30-10) were rotated for 3 h at 4°C and washed 4-5 times with the reaction buffer. The bound proteins were separated by SDS-PAGE and detected by immunoblot with anti-Flag antibody (Abmart, cat#M20008L).

Binding assays

Binding assays were performed as previously described with modifications.[39,76,77] Anti-Flag® M2 agarose beads (Sigma-Aldrich, cat#A2220) immunoadsorbed with SYR1^{Ecto}-HA-Flag and SYR2^{Ecto}-HA-Flag were washed twice with extraction buffer (50 mM pH 7.5 Tris-HCl, 150 mM NaCl, 0.2% [v/v] Triton X-100, 0.2% [v/v] NP-40, 10 mM DTT) containing 1× protease inhibitor cocktail (Roche, cat#05056489001), followed by two washes with binding buffer (25 mM MES, pH 6.0, 10 mM NaCl, 3 mM $MgCl_2$, and 0.2% [v/v] Triton X-100). Beads were resuspended in binding buffer (10 μl beads per 100 μl total volume) and incubated with acrisystemin alone or with various concentrations of unlabeled peptides as competitors. After 30 minutes of incubation on a rotator in a cold room, unbound ligands were removed by two rounds of rapid washing with 1 ml of binding buffer. Beads were resuspended in 100 μl of 5 mM citric acid, and acridinium ester emission was measured using an EnSpire multimode plate reader (PerkinElmer) after adding 150 μl of reacting solution with 100 mM NaOH and 20 mM H_2O_2.

Expression and purification of SYR1^{Ecto} and SYR2^{Ecto} for MST analysis

SYR1^{Ecto} (1-2340 bp) and *SYR2^{Ecto}* (1-2325 bp) were cloned into the pEAQ-HT vector[78] with a C-terminal 3×Flag-6×His tag to generate the *SYR1^{Ecto}-Flag-His* and *SYR2^{Ecto}-Flag-His* constructs. The resulting expression vectors were transformed into *A. tumefaciens* GV3101 and infiltrated into *N. benthamiana* leaves. After 3 days of growth under normal condition in a growth chamber, the infiltrated leaves were ground in extraction buffer (50 mM pH7.5 Tris-HCl, 150 mM NaCl, 0.1% [v/v] TritonX-100, 0.2% [v/v] NP-40,10 mM DTT) containing 1×protease inhibitor cocktail (Roche, cat#05056489001). The sample was incubated with anti-FLAG affinity resin (Genscript, cat#L00766) on a rotator at 4 °C for 5 hours, then washed with extraction buffer and subsequently eluted with PBS buffer (8 g/L NaCl, 0.2 g/L KCl, 1.42 g/L Na2HPO4, 0.27 g/L KH2PO4, pH 7.4) containing 500 μg/mL FLAG (DYKDDDDK) peptide. The eluted fractions were further purified by size-exclusion chromatography (Hiload 16/600 Superdex 200 prep grade, GE Healthcare) in a 10 mM Bis-Tris pH 6.0, 100 mM NaCl buffer. Fractions containing SYR1^{Ecto}-Flag-His and SYR2^{Ecto}-Flag-His were collected and concentrated.

Expression and purification of SERK3a^{Ecto} for MST analysis

The codon-optimized *SERK3a^{Ecto}* (1-660 bp) was cloned into a modified pFastBac1 vector (Invitrogen) with a C-terminal 6×His-tag as previously described.[79] The resulting construct was expressed in HIGH FIVE insect cells (Invitrogen) and purified as described.[80]

Please cite this article in press as: Zhou et al., Antagonistic systemin receptors integrate the activation and attenuation of systemic wound signaling in tomato, Developmental Cell (2024), https://doi.org/10.1016/j.devcel.2024.11.005

Briefly, one liter of insect cells (2.0×10^6 cells/mL) was infected with 25 mL recombinant baculovirus. Sixty hours after infection, the media were harvested and affinity-purified with Ni-NTA (Novagen, cat#70666). The protein elution was further purified by size-exclusion chromatography (Hiload 16/600 Superdex 200 prep grade, GE Healthcare) in a 10 mM Bis-Tris pH 6.0, 100 mM NaCl buffer.

Microscale thermophoresis (MST) assay

MST assays to quantify the binding affinity of $SYR1^{Ecto}$ or $SYR2^{Ecto}$ with $SERK3a^{Ecto}$ was conducted using Monolith NT.115 (Nanotemper Technologies) as previously described.[79] $SYR1^{Ecto}$ and $SYR2^{Ecto}$ were labeled with the RED fluorescent dye NT-647-NHS using the Monolith™ Protein Labeling Kit MO-L001. The prepared systemin-$SYR1^{Ecto}$ or systemin-$SYR2^{Ecto}$ complexes were mixed with unlabeled $SERK3a^{Ecto}$ diluted to appropriate serial concentrations in buffer containing 10 mM Bis-Tris pH 6.0, 100 mM NaCl. The final concentration of target ($SYR1^{Ecto}$-Flag-His, $SYR2^{Ecto}$-Flag-His) is 100 nM and the final gradient-diluted ligand ($SERK3a^{Ecto}$-His) concentrations are ranging from 0.000916 to 30 μM. The samples were loaded into the silica capillaries (Monolith™ Standard Treated Capillaries, Cat#MO-K022) and measurements were performed using medium MST power and 100% LED power at room temperature. Raw data was further analyzed by MO. Affinity Analysis software. Data points in Figure 6F indicate the difference in normalized fluorescence (‰) generated by $SYR1^{Ecto}$ and $SYR2^{Ecto}$ with $SERK3a^{Ecto}$ or systemin-saturated-$SYR1^{Ecto}$and $SYR2^{Ecto}$ with $SERK3a^{Ecto}$. All assays were repeated for three times to ensure reproducibility.

Chromatin immunoprecipitation–quantitative polymerase chain reaction (ChIP-qPCR)

ChIP assays were performed as previously described.[36,51] Briefly, 18-d-old *MYC2-GFP-9* seedlings were wounded with a hemostat and incubated under continuous light for 30 min. Then, 5 g of leaf tissue was harvested and cross-linked with 1% (v/v) formaldehyde under a vacuum for 10 min. Cross-linking was quenched in 0.125 M glycine under vacuum for 5 min. Quenched samples were washed three times and then the chromatin complex was isolated, resuspended in lysis buffer (10 mM Tris-HCl [pH 8.0], 20 mM EDTA, 400 mM NaCl, 1% [v/v] Triton X-100, 2 mM PMSF) containing 1× protease inhibitor cocktail (Roche, cat#05056489001), and sheared by sonication to reduce the average DNA fragment size to ~500 bp. Then, 50 μL of the sheared chromatin was saved for use as the input control. GFP antibody (Abcam, cat#AB290) was incubated with Dynabeads™ Protein G (Invitrogen, cat#10004D) at 4°C for at least 6 h and added to the remaining chromatin for incubation at 4°C overnight. The immunoprecipitated chromatin complex was successively washed with low-salt buffer (20 mM Tris-HCl [pH 8.0], 2 mM EDTA, 150 mM NaCl, 0.5% [v/v] Triton X-100, and 0.2% [w/v] SDS), high-salt buffer (20 mM Tris-HCl [pH 8.0], 2 mM EDTA, 500 mM NaCl, 0.5% [v/v] Triton X-100, and 0.2% [w/v] SDS), LiCl buffer (10 mM Tris-HCl [pH 8.0], 1 mM EDTA, 0.25 M LiCl, 0.5% [v/v] NP-40, and 0.5% [w/v] sodium deoxycholate), and TE buffer (10 mM Tris-HCl [pH 8.0] and 1 mM EDTA). After washing, the immunoprecipitated chromatin was eluted with elution buffer (1% [w/v] SDS and 0.1 M $NaHCO_3$). Protein–DNA cross linking was reversed by incubating the immunoprecipitated complexes with 20 mL 5 M NaCl at 65°C overnight. DNA was recovered using a QIAquick PCR Purification Kit (Qiagen, cat#28106) and analyzed by qPCR using the respective primer pairs (Table S1). ChIP signals were displayed as the percentage of precipitated DNA relative to input DNA. The fold enrichment on selected regions was normalized against the non-specific binding region of the *ACTIN2* (Solyc11g005330) promoter. Each PCR was repeated three times, and the mean value of technical replicates was recorded for each biological replicate. Error bars represent the SD from three independent experiments.

Electrophoretic mobility shift assay (EMSA)

EMSA was performed as described previously.[36,51] Briefly, the recombinant MBP-MYC2 fusion proteins were expressed in *E. coli* BL21 (DE3) cells and affinity-purified with amylase resin (New England Biolabs, cat# E8021L), according to manufacturer's instructions. Oligonucleotide probes were synthesized and labeled with biotin at the 5' end by Invitrogen. EMSA was performed using a Chemiluminescent EMSA kit (Beyotime, cat#GS009). Biotin-labeled probes were incubated with MBP-MYC2 fusion proteins at room temperature for 20 min, free and bound probes were separated in an acrylamide gel. Mutated probes, in which the G-box-like motif (5'-CACGTT-3') /G-box-like variant (5'-CACTTG-3') was replaced by 5'-AAAAAA-3', were used as negative controls. Unlabeled wild type and mutated probes were used as competitors. Probes used for EMSA are listed in Table S1.

In vitro and *in vivo* phosphorylation assays

GST-tagged recombinant proteins were expressed in *E. coli* strain BL21 and affinity-purified with GST Bind Resin (Merck Millipore, cat#70541-4), according to manufacturer's instructions. The *in vitro* phosphorylation assays were performed as described.[64] In brief, 2 μg purified fusion proteins of the indicated constructs were incubated in protein kinase assay buffer (50 mM HEPES pH 7.5, 5 mM $MgCl_2$, 1 mM DTT, 1 μCi [γ-^{32}P] ATP, 100 μM ATP) for 30 min at 25°C. The phosphorylated proteins were analyzed by 10% SDS-PAGE and detected by Typhoon FLA9500 imager (General Electric Company). Coomassie Brilliant Blue staining was used as a loading control.

In vivo phosphorylation assays were performed as described previously with modifications.[81] Briefly, *A. tumefaciens* strains GV3101 containing indicated constructs were infiltrated into fully expanded leaves of *N. benthamiana* plants. After incubation for 72 h, the infiltrated leaves were infiltrated with 100 nM systemin or H_2O for 20 min, then the plant materials were ground in liquid nitrogen, and extracted with buffer [50 mM Tris-HCl, pH 7.5; 150 mM NaCl, 5 mM EDTA, 0.2% NP40, 0.3% Triton X-100, 10 mM DTT, 1% (vol/vol) protease inhibitor mixture, phosphatase inhibitor 2 and 3 (Sigma)]. Samples were centrifuged and supernatants incubated 4 h at 4°C with anti-Flag® M2 agarose beads (Sigma-Aldrich, cat#A2220). Following incubation, the beads were collected and washed four times with the extraction buffer. Immunoprecipitates were finally incubated 30 min at 30°C and under vigorous

shaking with 30 μL of the kinase buffer (50 mM Tris-HCl, pH 7.5, 1 mM DTT, 10 mM $MgCl_2$, 100 μM ATP, 0.3 μCi [γ-^{32}P] -ATP). The reactions were stopped by addition of SDS loading buffer and denatured for 5 min at 95°C. The phosphorylated proteins were analyzed by 10% SDS-PAGE and detected by Typhoon FLA9500 imager (General Electric Company). Densitometry measurements were carried out with the Image J software.

Oxidative burst assays

ROS measurement was performed as described with modifications.[82] For systemin-induced ROS burst in tomato leaves, fully expanded leaves of 18-d-old seedlings were punched into 4 mm-diameter leaf discs and floated overnight on sterile water in a 96-well plate. For systemin-induced ROS burst in *N. benthamiana* leaves, *A. tumefaciens* strains containing the desired constructs were infiltrated into fully expanded leaves of 6-week-old *N. benthamiana* plants, and then incubated for 72 h. Leaves were punched into 4 mm-diameter leaf discs and floated overnight on sterile water in a 96-well plate. After 12 h incubation, the water was replaced with a solution of 20 μM L-012 (Wako, cat#120-04891) and 2 μg/mL horseradish peroxidase (Sigma-Aldrich, cat#P6782) containing 100 nM systemin or 100 nM flg22. Luminescence was recorded using the EnSpire multimode plate reader (PerkinElmer). Each data point consists at least 6 leaf discs.

MAPK activation assays

To investigate systemin-induced MAPK activation in tomato leaves, 18-d-old tomato seedlings of the indicated genotypes were excised at the base of the stem and placed in 0.5 mL microfuge tubes containing 400 μL of water. After 4 h incubation (wound-induced MAPK activation was reduced to basal level), plants were transferred to 1.5 mL microfuge tubes containing 100 nM systemin or 100 nM flg22 for 30 min. Leaf tissues of five plants were pooled for protein extraction. MAPK activation was detected by immunoblotting analysis with an anti-pERK antibody (Cell Signaling, cat#4370), and the RubisCO bands were stained with Ponceau as the loading control.

To investigate systemin-induced MAPK activation in *N. benthamiana*, *A. tumefaciens* strains containing the desired constructs were infiltrated into fully expanded leaves of *N. benthamiana* plants. After incubation for 72 h, the *N. benthamiana* leaves treated with or without 100 nM systemin for 20 min. MAPK activation was detected by immunoblotting analysis with an anti-pERK antibody (Cell Signaling, cat#4370), and SYR-Flag as the loading control. Densitometry measurements were carried out with the Image J software.

Transient expression in leaf mesophyll protoplasts of Arabidopsis

Transformation of Arabidopsis leaf mesophyll protoplasts and monitoring of the *pFRK1*::Luciferase reporter were performed as described with slight modifications.[47,77] Briefly, desired plasmids in the *pUC19-35S-Flag-RBS* vector were co-transfected with *FRK1::LUC* (firefly luciferase) and *35S::Ren-LUC* (Renilla luciferase) into Arabidopsis protoplasts. The protoplasts were incubated overnight under low light, treated with indicated concentration of systemin for 3 h. Protein was then isolated, and LUC activity was recorded using a GLOMAX 96 microplate luminometer (Promega) with the Dual-Luciferase Reporter Assay System (Promega, cat#E1910) according to the manufacturer's instructions.

QUANTIFICATION AND STATISTICAL ANALYSIS

Significance of difference was examined by two-tailed Student's t test (*$p < 0.05$; **$p < 0.01$; ***$p < 0.001$; ns, not significant). For the proteins quantification, band intensity was performed using the ImageJ.

Developmental Cell, Volume *60*

Supplemental information

Antagonistic systemin receptors integrate the activation and attenuation of systemic wound signaling in tomato

Ke Zhou, Fangming Wu, Lei Deng, Yu Xiao, Wentao Yang, Jiuhai Zhao, Qinyang Wang, Zeqian Chang, Huawei Zhai, Chuanlong Sun, Hongyu Han, Minmin Du, Qian Chen, Jijun Yan, Peiyong Xin, Jinfang Chu, Zhifu Han, Jijie Chai, Gregg A. Howe, Chang-Bao Li, and Chuanyou Li

Supplemental information

Antagonistic systemin receptors integrate the attenuation with activation of systemic wound signaling in tomato

Ke Zhou, Fangming Wu, Lei Deng, Yu Xiao, Wentao Yang, Jiuhai Zhao, Qinyang Wang, Zeqian Chang, Huawei Zhai, Chuanlong Sun, Hongyu Han, Minmin Du, Qian Chen, Jijun Yan, Peiyong Xin, Jinfang Chu, Zhifu Han, Jijie Chai, Gregg A. Howe, Chang-Bao Li and Chuanyou Li

Figure S1.

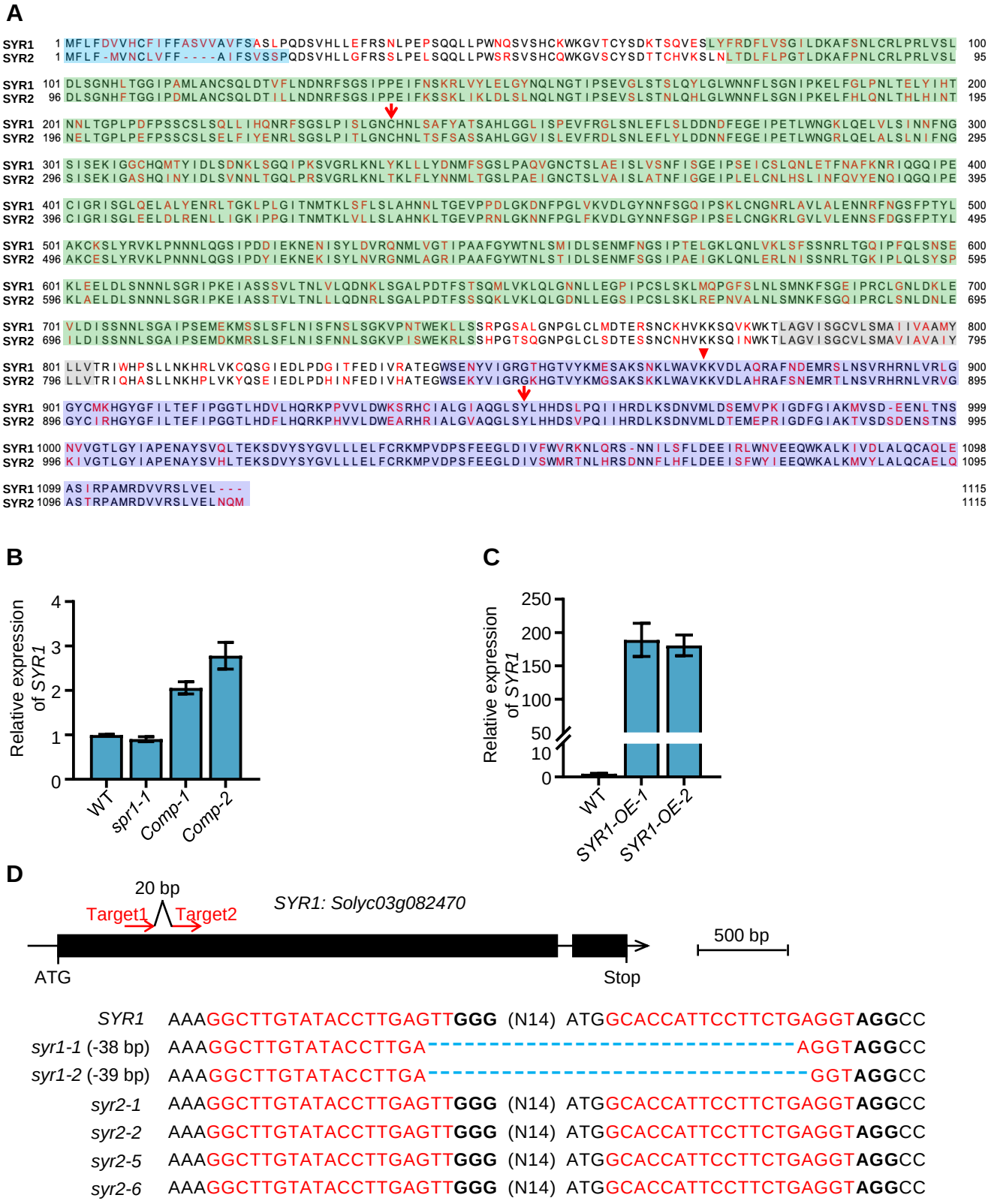
A
SYR1 1 MFLFDVVHCFIFFASVVAVFSASLPQDSVHLLEFRSNLPEPSQQLLPWNQSVSHCKWKGVTCYSDKTSQVESLYFRDFLVSGILDKAFSNLCRLPRLVSL 100
SYR2 1 MFLF-MVNCLVFF----AIFSVSSPQDSVHLLGFRSSLPELSQQLLPWSRSVSHCQWKGVSCYSDTTCHVKSLNLTDLFLPGTLDKAFPNLCRLPRLVSL 95
SYR1 101 DLSGNHLTGGIPAMLANCSQLDTVFLNDNRFSGSIPPEIFNSKRLVYLELGYNQLNGTIPSEVGLSTSLQYLGLWNNFLSGNIPKELFGLPNLTELYIHT 200
SYR2 96 DLSGNHFTGGIPDMLANCSQLDTILLNDNRFSGSIPPEIFKSSKLIKLDLSLNQLNGTIPSEVSLSTNLQHLGLWNNFLSGNIPKELFHLQNLTHLHINT 195
SYR1 201 NNLTGPLPDFPSSCSLSQLLIHQNRFSGSLPISLGNCHNLSAFYATSAHLGGLISPEVFRGLSNLEFLSLDDNDFEGEIPETLWNGKLQELVLSINNFNG 300
SYR2 196 NELTGPLPEFPSSCSLSELFIYENRLSGSLPITLGNCHNLTSFSASSAHLGGVISLEVFRDLSNLEFLYLDDNNFEGEIPETLWNGRLQELALSLNIFNG 295
SYR1 301 SISEKIGGCHQMTYIDLSDNKLSGQIPKSVGRLKNLYKLLLYDNMFSGSLPAQVGNCTSLAEISLVSNFISGEIPSEICSLQNLETFNAFKNRIQGQIPE 400
SYR2 296 SISEKIGASHQINYIDLSVNNLTGQLPRSVGRLKNLTKLFLYNNMLTGSLPAEIGNCTSLVAISLATNFIGGEIPLELCNLHSLINFQVYENQIQGQIPE 395
SYR1 401 CIGRISGLQELALYENRLTGKLPLGITNMTKLSFLSLAHNNLTGEVPPDLGKDNFPGLVKVDLGYNNFSGQIPSKLCNGNRLAVLALENNRFNGSFPTYL 500
SYR2 396 CIGRISGLEELDLRENLLIGKIPPGITNMTKLVLLSLAHNKLTGEVPRNLGKNNFPGLFKVDLGYNNFSGPIPSELCNGKRLGVLVLENNSFDGSFPTYL 495
SYR1 501 AKCKSLYRVKLPNNNLQGSIPDDIEKNENISYLDVRQNMLVGTIPAAFGYWTNLSMIDLSENMFNGSIPTELGKLQNLVKLSFSSNRLTGQIPFQLSNSE 600
SYR2 496 AKCESLYRVKLPNNNLQGSIPDYIEKNEKISYLNVRGNMLAGRIPAAFGYWTNLSTIDLSENMFSGSIPAEIGKLQNLERLNISSNRLTGKIPLQLSYSP 595
SYR1 601 KLEELDLSNNNLSGRIPKEIASSSVLTNLVLQDNKLSGALPDTFSTSQMLVKLQLGNNLLEGPIPCSLSKLMQPGFSLNLSMNKFSGEIPRCLGNLDKLE 700
SYR2 596 KLAELDLSNNNLSGRIPKEIASSTVLTNLLLQDNRLSGALPDTFSSSQKLVKLQLGDNLLEGSIPCSLSKLREPNVALNLSMNKFSGQIPRCLSNLDNLE 695
SYR1 701 VLDISSNNLSGAIPSEMEKMSSLSFLNISFNSLSGKVPNTWEKLLSSRPGSALGNPGLCLMDTERSNCKHVKKSQVKWKTLAGVISGCVLSMAIIVAAMY 800
SYR2 696 ILDISSNNLSGAIPSEMDKMRSLSFLNISFNNLSGKVPISWEKRLSSHPGTSQGNPGLCLSDTESSNCNHVKKSQINWKTLAGVISGCVLSMAVIAVAIY 795
SYR1 801 LLVTRIWHPSLLNKHRLVKCQSGIEDLPDGITFEDIVRATEGWSENYVIGRGTHGTVYKMESAKSNKLWAVKKVDLAQRAFNDEMRSLNSVRHRNLVRLG 900
SYR2 796 LLVTRIQHASLLNKHPLVKYQSEIEDLPDHINFEDIVHATEGWSEKYVIGRGKHGTVYKMGSAKSKKLWAVKKVDLAHRAFSNEMRTLNSVRHRNLVRVG 895
SYR1 901 GYCMKHGYGFILTEFIPGGTLHDVLHQRKPPVVLDWKSRHCIALGIAQGLSYLHHDSLPQIIHRDLKSDNVMLDSEMVPKIGDFGIAKMVSD-EENLTNS 999
SYR2 896 GYCIRHGYGFILTEFIPGGTLHDFLHQRKPHVVLDWEARHRIALGVAQGLSYLHHDSVPQIIHRDLKSDNVMLDTEMEPRIGDFGIAKTVSDSDENSTNS 995
SYR1 1000 NVVGTLGYIAPENAYSVQLTEKSDVYSYGVLLLELFCRKMPVDPSFEEGLDIVFWVRKNLQRS-NNILSFLDEEIRLWNVEEQWKALKIVDLALQCAQLE 1098
SYR2 996 KIVGTLGYIAPENAYSVHLTEKSDVYSYGVLLLELFCRKMPVDPSFEEGLDIVSWMRTNLHRSDNNFLHFLDEEISFWYIEEQWKALKMVYLALQCAELQ 1095
SYR1 1099 ASIRPAMRDVVRSLVEL--- 1115
SYR2 1096 ASTRPAMRDVVRSLVELNQM 1115
B
Relative expression of SYR1
0
1
2
3
4
WT
spr1-1
Comp-1
Comp-2
C
Relative expression of SYR1
0
10
50
100
150
200
250
WT
SYR1-OE-1
SYR1-OE-2
D
20 bp
Target1
Target2
SYR1: Solyc03g082470
500 bp
ATG
Stop
SYR1 AAAGGCTTGTATACCTTGAGTTGGG (N14) ATGGCACCATTCCTTCTGAGGTAGGCC
syr1-1 (-38 bp) AAAGGCTTGTATACCTTGA----------AGGTAGGCC
syr1-2 (-39 bp) AAAGGCTTGTATACCTTGA----------GGTAGGCC
syr2-1 AAAGGCTTGTATACCTTGAGTTGGG (N14) ATGGCACCATTCCTTCTGAGGTAGGCC
syr2-2 AAAGGCTTGTATACCTTGAGTTGGG (N14) ATGGCACCATTCCTTCTGAGGTAGGCC
syr2-5 AAAGGCTTGTATACCTTGAGTTGGG (N14) ATGGCACCATTCCTTCTGAGGTAGGCC
syr2-6 AAAGGCTTGTATACCTTGAGTTGGG (N14) ATGGCACCATTCCTTCTGAGGTAGGCC

Figure S1. *SPR1* encodes the systemin receptor SYR1, related to Figure 2

(A) Protein sequence alignment between SYR1 and SYR2. Protein sequences were aligned and visualized by program Jalview (version, 2.1.1, https://www.jalview.org/). Protein domains were predicted by InterPro (http://www.ebi.ac.uk/interpro/). The leucine-rich-repeat (LRR) domain was predicted based on the consensus LRR sequences (xLxxLxLxxNxLS/TGxIPxxLGxLx). Blue box, signal peptide; Green box, LRR domain; Grey box, transmembrane domain; Purple box, kinase domain. Arrowheads indicate $SYR1^{C237}$ and $SYR1^{Y952}$. Triangles indicate $SYR1^{K872}$ and $SYR2^{K867}$.

(B) RT-qPCR showing *SYR1* expression in indicated *spr1-1* complementation plants (*Comp*). The error bars represent SD, data are mean ± SD, *n* = 3 repeats. CM was used as WT.

(C) RT-qPCR showing *SYR1* expression in indicated *SYR1-OE* lines. The error bars represent SD, data are mean ± SD, *n* = 3 repeats. AC was used as WT.

(D) CRISPR/Cas9-mediated editing of *SYR1*. *SYR1* exons are targeted by two sgRNAs. sgRNA target (red) and PAM (bold) sequences are indicated. Blue dashes indicate deletions, numbers indicate the number of nucleotides involved.

Figure S2.

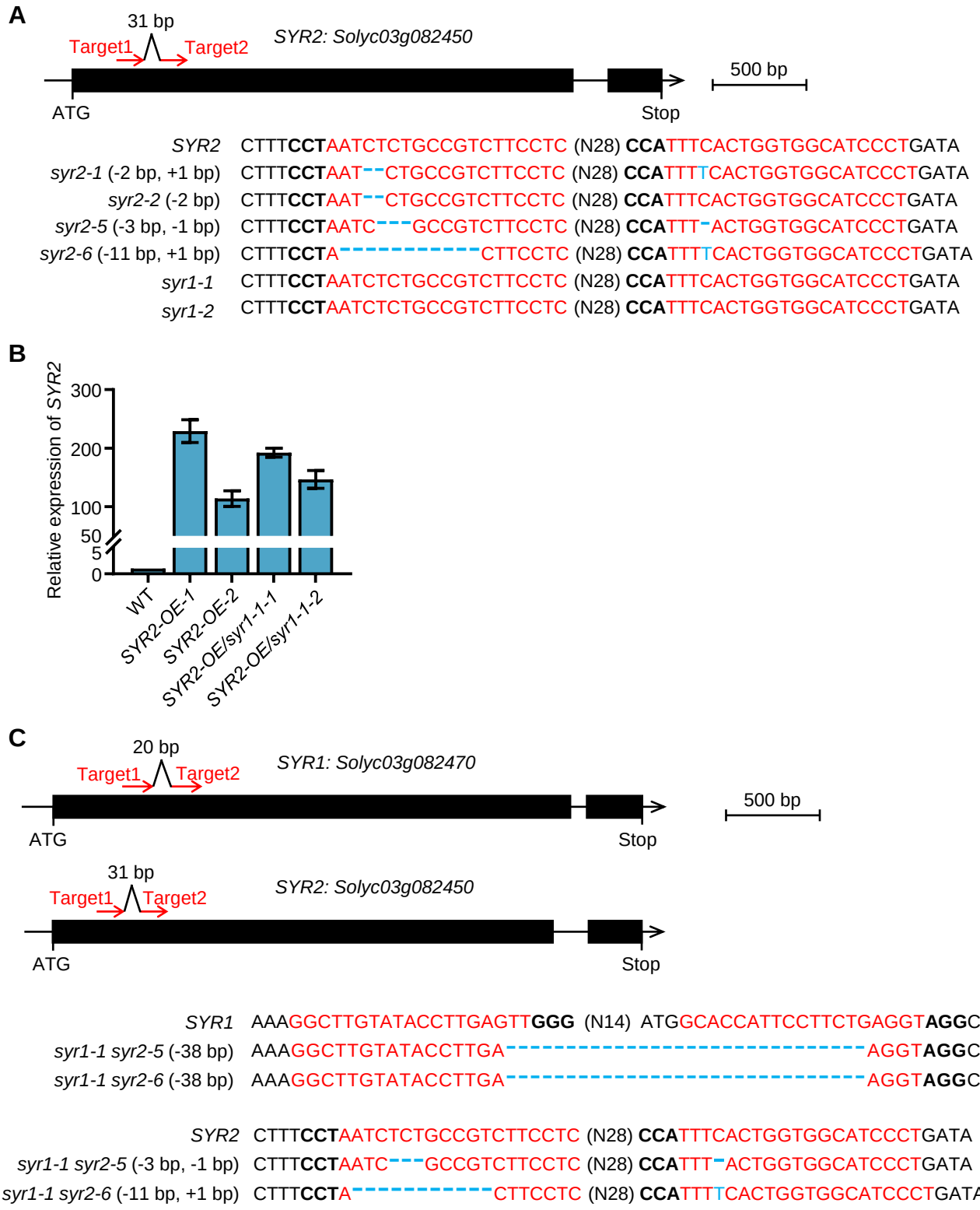
A
31 bp
Target1
Target2
SYR2: Solyc03g082450
500 bp
ATG
Stop
SYR2 CTTTCCTAATCTCTGCCGTCTTCCTC (N28) CCATTTCACTGGTGGCATCCCTGATA
syr2-1 (-2 bp, +1 bp) CTTTCCTAAT--CTGCCGTCTTCCTC (N28) CCATTTTCACTGGTGGCATCCCTGATA
syr2-2 (-2 bp) CTTTCCTAAT--CTGCCGTCTTCCTC (N28) CCATTTCACTGGTGGCATCCCTGATA
syr2-5 (-3 bp, -1 bp) CTTTCCTAATC---GCCGTCTTCCTC (N28) CCATTT-ACTGGTGGCATCCCTGATA
syr2-6 (-11 bp, +1 bp) CTTTCCTA----------CTTCCTC (N28) CCATTTTCACTGGTGGCATCCCTGATA
syr1-1 CTTTCCTAATCTCTGCCGTCTTCCTC (N28) CCATTTCACTGGTGGCATCCCTGATA
syr1-2 CTTTCCTAATCTCTGCCGTCTTCCTC (N28) CCATTTCACTGGTGGCATCCCTGATA
B
Relative expression of SYR2
300
200
100
50
5
0
WT
SYR2-OE-1
SYR2-OE-2
SYR2-OE/syr1-1-1
SYR2-OE/syr1-1-2
C
20 bp
Target1
Target2
SYR1: Solyc03g082470
500 bp
ATG
Stop
31 bp
Target1
Target2
SYR2: Solyc03g082450
ATG
Stop
SYR1 AAAGGCTTGTATACCTTGAGTTGGG (N14) ATGGCACCATTCCTTCTGAGGTAGGCC
syr1-1 syr2-5 (-38 bp) AAAGGCTTGTATACCTTGA----------AGGTAGGCC
syr1-1 syr2-6 (-38 bp) AAAGGCTTGTATACCTTGA----------AGGTAGGCC
SYR2 CTTTCCTAATCTCTGCCGTCTTCCTC (N28) CCATTTCACTGGTGGCATCCCTGATA
syr1-1 syr2-5 (-3 bp, -1 bp) CTTTCCTAATC---GCCGTCTTCCTC (N28) CCATTT-ACTGGTGGCATCCCTGATA
syr1-1 syr2-6 (-11 bp, +1 bp) CTTTCCTA----------CTTCCTC (N28) CCATTTTCACTGGTGGCATCCCTGATA

Figure S2. Generation of *syr2* mutants, *SYR2-OE* plants and *syr1 syr2* double mutants, related to Figure 3

(A) CRISPR/Cas9-mediated editing of *SYR2*. *SYR2* exons are targeted by two sgRNAs. sgRNA target (red) and PAM (bold) sequences are indicated. Blue dashes and letters indicate deletions and insertions, respectively, numbers indicate the number of nucleotides involved (+, insertion; -, deletion).

(B) RT-qPCR analysis showing *SYR2* expression levels of different *SYR2*-overexpression plants in the background of WT (*SYR2-OE*) or *syr1-1* (*SYR2-OE/syr1-1*). The error bars represent SD, data are mean ± SD, n = 3 repeats.

(C) CRISPR/Cas9-mediated editing of *SYR1* and *SYR2*. Exons of target genes are targeted by CRISPR/Cas9 using two sgRNAs. sgRNA target (red) and PAM (bold) sequences are indicated. Blue dashes and letters indicate deletions and insertions, respectively, and the numbers in parentheses indicate the number of nucleotides involved (+, insertion; -, deletion).

Figure S3.

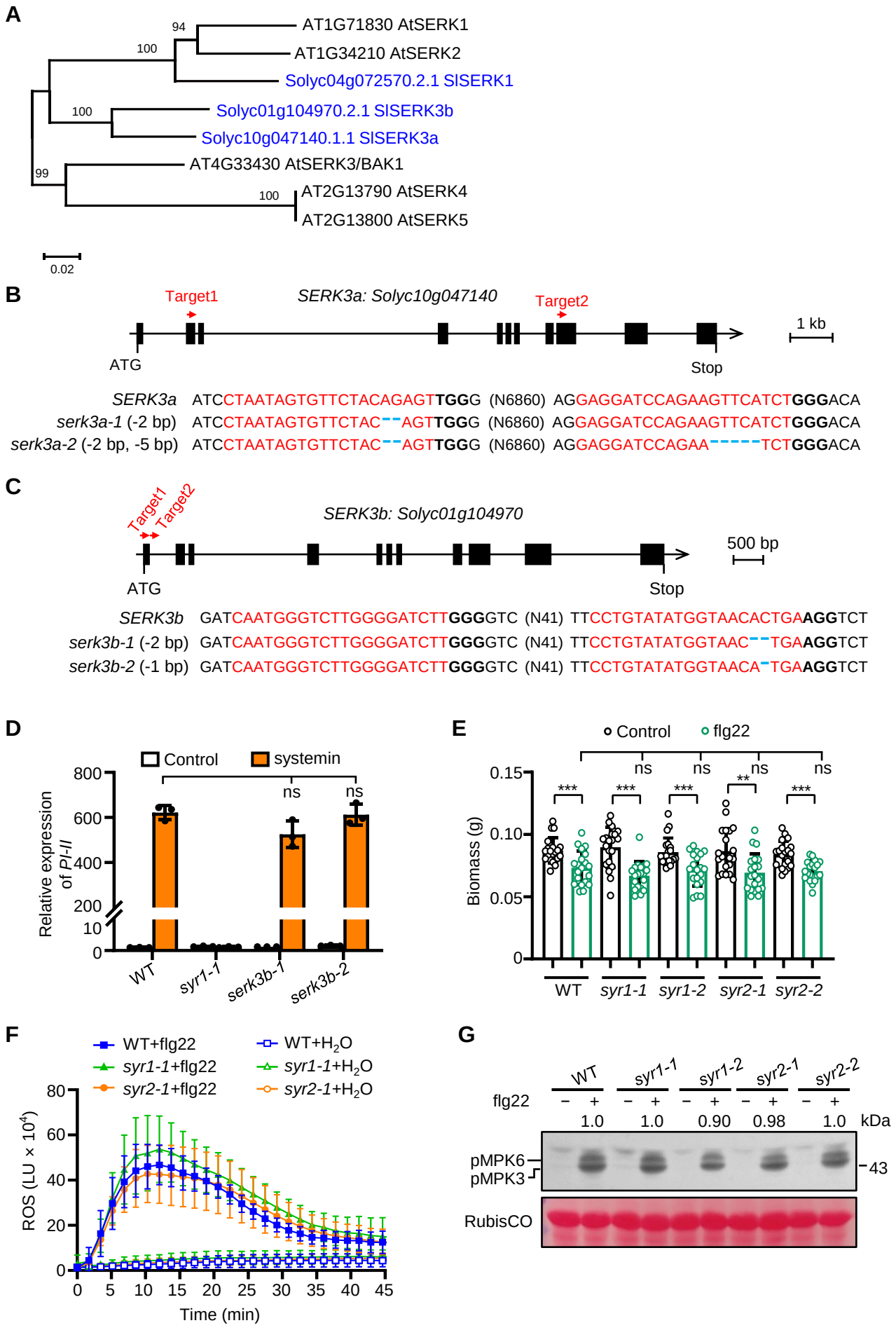
A
94
100
100
99
100
AT1G71830 AtSERK1
AT1G34210 AtSERK2
Solyc04g072570.2.1 SlSERK1
Solyc01g104970.2.1 SlSERK3b
Solyc10g047140.1.1 SlSERK3a
AT4G33430 AtSERK3/BAK1
AT2G13790 AtSERK4
AT2G13800 AtSERK5
0.02
B
Target1
SERK3a: Solyc10g047140
Target2
1 kb
ATG
Stop
SERK3a ATCCTAATAGTGTTCTACAGAGTTGGG (N6860) AGGAGGATCCAGAAGTTCATCTGGGACA
serk3a-1 (-2 bp) ATCCTAATAGTGTTCTAC--AGTTGGG (N6860) AGGAGGATCCAGAAGTTCATCTGGGACA
serk3a-2 (-2 bp, -5 bp) ATCCTAATAGTGTTCTAC--AGTTGGG (N6860) AGGAGGATCCAGAA-----TCTGGGACA
C
Target1
Target2
SERK3b: Solyc01g104970
500 bp
ATG
Stop
SERK3b GATCAATGGGTCTTGGGGATCTTGGGGTC (N41) TTCCTGTATATGGTAACACTGAAGGTCT
serk3b-1 (-2 bp) GATCAATGGGTCTTGGGGATCTTGGGGTC (N41) TTCCTGTATATGGTAAC--TGAAGGTCT
serk3b-2 (-1 bp) GATCAATGGGTCTTGGGGATCTTGGGGTC (N41) TTCCTGTATATGGTAACA-TGAAGGTCT
D
Control
systemin
Relative expression of PI-II
800
600
400
200
10
0
ns
ns
WT
syr1-1
serk3b-1
serk3b-2
E
Control
flg22
Biomass (g)
0.15
0.10
0.05
0
ns
***
**
WT
syr1-1
syr1-2
syr2-1
syr2-2
F
WT+flg22
syr1-1+flg22
syr2-1+flg22
WT+H2O
syr1-1+H2O
syr2-1+H2O
ROS (LU × 10^4)
80
60
40
20
0
0 5 10 15 20 25 30 35 40 45
Time (min)
G
WT
syr1-1
syr1-2
syr2-1
syr2-2
flg22
1.0
1.0
0.90
0.98
1.0
kDa
pMPK6
pMPK3
43
RubisCO

Figure S3. SERK3a complexes with SYR1 and SYR2 in response to systemin, related to Figure 6

(A) Phylogenetic tree of *Arabidopsis thaliana* SERKs (in black) and their tomato orthologs (in blue) on the basis of protein sequences. The phylogenetic tree was constructed by Neighbor-joining Method. Bootstrap values for 1000 replicates are indicated at the forks. The scale bar indicates the average number of amino acid substitutions per site.

(B) CRISPR/Cas9-mediated editing of *SERK3a*. *SERK3a* exons are targeted by two sgRNAs. sgRNA target (red) and PAM (bold) sequences are indicated. Blue dashes indicate deletions, numbers indicate the number of nucleotides involved.

(C) CRISPR/Cas9-mediated editing of *SERK3b*. *SERK3b* exons are targeted by two sgRNAs. sgRNA target (red) and PAM (bold) sequences are indicated. Blue dashes indicate deletions, numbers indicate the number of nucleotides involved.

(D) Systemin-induced *PI-II* expression in indicated genotypes. Eighteen-d-old seedlings were treated with or without 100 nM systemin. *PI-II* levels were measured 12 hours after treatment. Data are mean ± SD, *n* = 3 repeats. ns, not significant (Student's *t* test).

(E) Biomass of 6-d-old seedlings of indicated genotypes grown on medium with or without 100 nM flg22. Data are mean ± SD, n = 20 seedlings.

(F) Flg22-induced ROS burst in indicated genotypes. Leaves from 18-d-old seedlings were treated with or without 100 nM flg22. ROS production was detected by luminometer over 45 min. LU, light units. Data are mean ± SD, n = 6 leaf discs.

(G) Flg22-triggered MPK3/6 activation in indicated genotypes. Eighteen-d-old seedlings of indicated genotypes were treated with 100 nM flg22 for 30 min before immunoblot with anti-pERK antibody. Ponceau staining of RubisCO indicates equal loading. Numbers indicate arbitrary densitometry units of pMPK3/6 normalized to the WT.

In (D) and (E), the error bars represent SD. **p <0.01, ***p <0.001 (Student's *t* test); ns, not significant.

Figure S4.

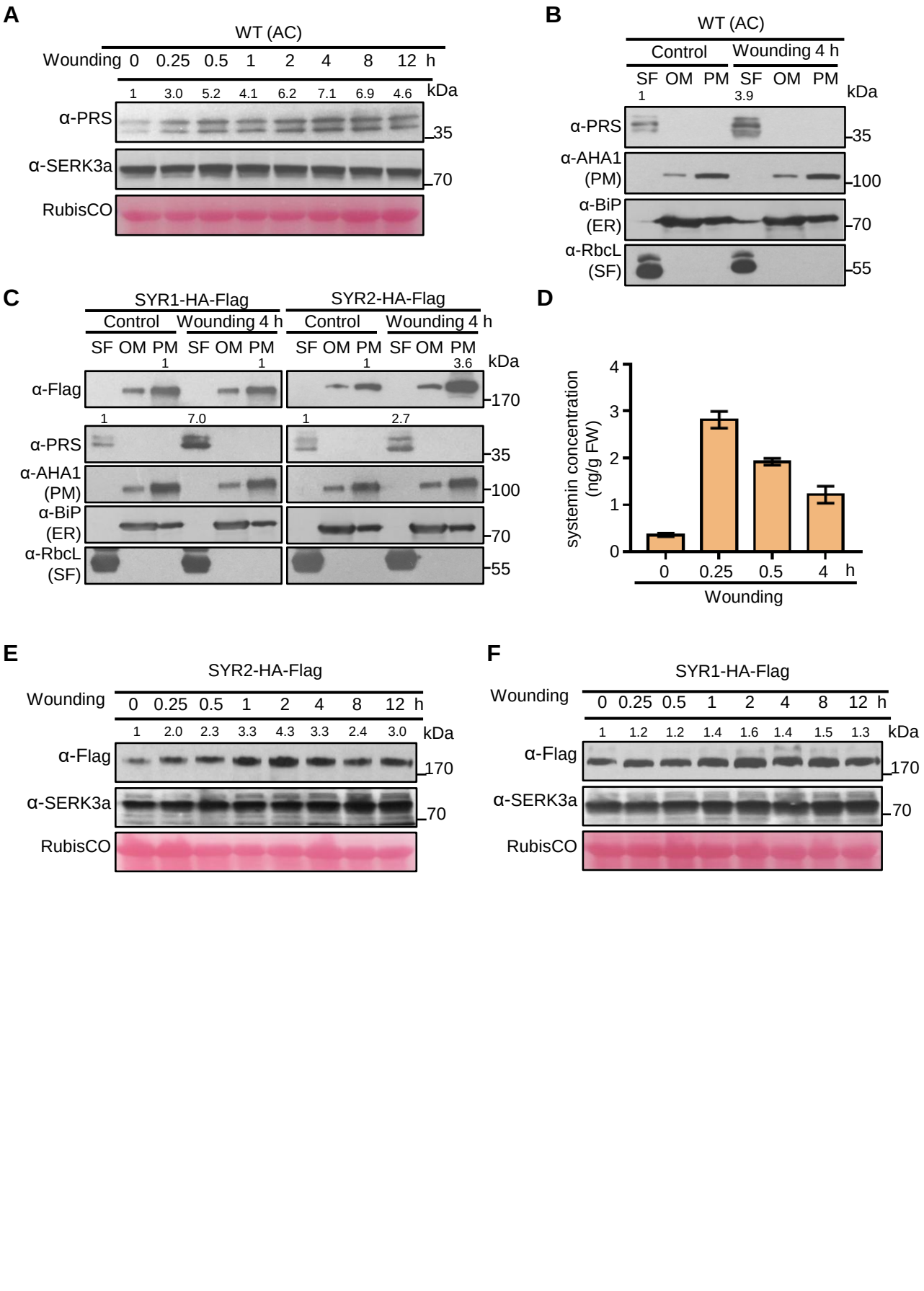
A
WT (AC)
Wounding 0 0.25 0.5 1 2 4 8 12 h
1 3.0 5.2 4.1 6.2 7.1 6.9 4.6
kDa
α-PRS
α-SERK3a
RubisCO
35
70
B
WT (AC)
Control
Wounding 4 h
SF OM PM SF OM PM
1 3.9
kDa
α-PRS
α-AHA1 (PM)
α-BiP (ER)
α-RbcL (SF)
35
100
70
55
C
SYR1-HA-Flag
SYR2-HA-Flag
Control
Wounding 4 h
SF OM PM SF OM PM SF OM PM SF OM PM
1 1 1 3.6
kDa
α-Flag
170
1 7.0 1 2.7
α-PRS
α-AHA1 (PM)
α-BiP (ER)
α-RbcL (SF)
35
100
70
55
D
systemin concentration (ng/g FW)
0 1 2 3 4
0 0.25 0.5 4 h
Wounding
E
SYR2-HA-Flag
Wounding 0 0.25 0.5 1 2 4 8 12 h
1 2.0 2.3 3.3 4.3 3.3 2.4 3.0
kDa
α-Flag
α-SERK3a
RubisCO
170
70
F
SYR1-HA-Flag
Wounding 0 0.25 0.5 1 2 4 8 12 h
1 1.2 1.2 1.4 1.6 1.4 1.5 1.3
kDa
α-Flag
α-SERK3a
RubisCO
170
70

Figure S4. Wounding differentially upregulates the protein abundance of SYR1, SYR2, SERK3a and PRS, related to Figure 7

(A) Wound-induced protein accumulation of PRS and SERK3a in WT plants. Eighteen-d-old WT seedlings were wounded and harvested at indicated time, prosystemin and SERK3a were detected by their antibodies. Numbers indicate band intensity normalized to untreated WT plants. Ponceau staining of RubisCO indicates equal loading. PRS, prosystemin.

(B) Subcellular fractionation analysis of prosystemin in WT. Eighteen-d-old WT seedlings were wounded, and leaf tissues were harvested for fractionation analysis 4 hours after wounding. Plasma membrane (PM), organelle membrane (OM) and soluble fraction (SF) were separated, and each fraction was probed with anti-prosystemin, anti-AHA1 (plasma membrane marker), anti-BiP (endoplasmic reticulum membrane marker), and anti-RbcL (soluble fraction marker). PRS, prosystemin.

(C) Subcellular fractionation analysis of SYR1-HA-Flag and SYR2-HA-Flag in indicated genotypes. Eighteen-d-old SYR1-HA-Flag or SYR2-HA-Flag seedlings were wounded, and leaf tissues were harvested for fractionation analysis 4 hours after wounding. Plasma membrane (PM), organelle membrane (OM) and soluble fraction (SF) were separated, and each fraction was probed with anti-Flag, anti-PRS, anti-AHA1 (plasma membrane marker), anti-BiP (endoplasmic reticulum membrane marker), and anti-RbcL (soluble fraction marker). PRS, prosystemin.

(D) Wound-induced accumulation of systemin in WT plants at indicated time. FW, fresh weight. The error bars represent SD, data are mean ± SD, n = 3 repeats.

(E) Wound-induced accumulation of the SYR2-HA-Flag fusion and SERK3a in *SYR2-HA-Flag* plants. SYR2-HA-Flag was detected by anti-Flag antibody and SERK3a was detected by anti-SERK3a antibody. Numbers indicate band intensity normalized to untreated *SYR2-HA-Flag* plants. Ponceau staining of RubisCO indicates equal loading.

(F) Wound-induced accumulation of the SYR1-HA-Flag fusion and SERK3a in *SYR1-HA-Flag* plants. SYR1-HA-Flag was detected by anti-Flag antibody and SERK3a was detected by anti-SERK3a antibody. Numbers indicate band intensity normalized to untreated *SYR1-HA-Flag* plants. Ponceau staining of RubisCO indicates equal loading.

Figure S5.

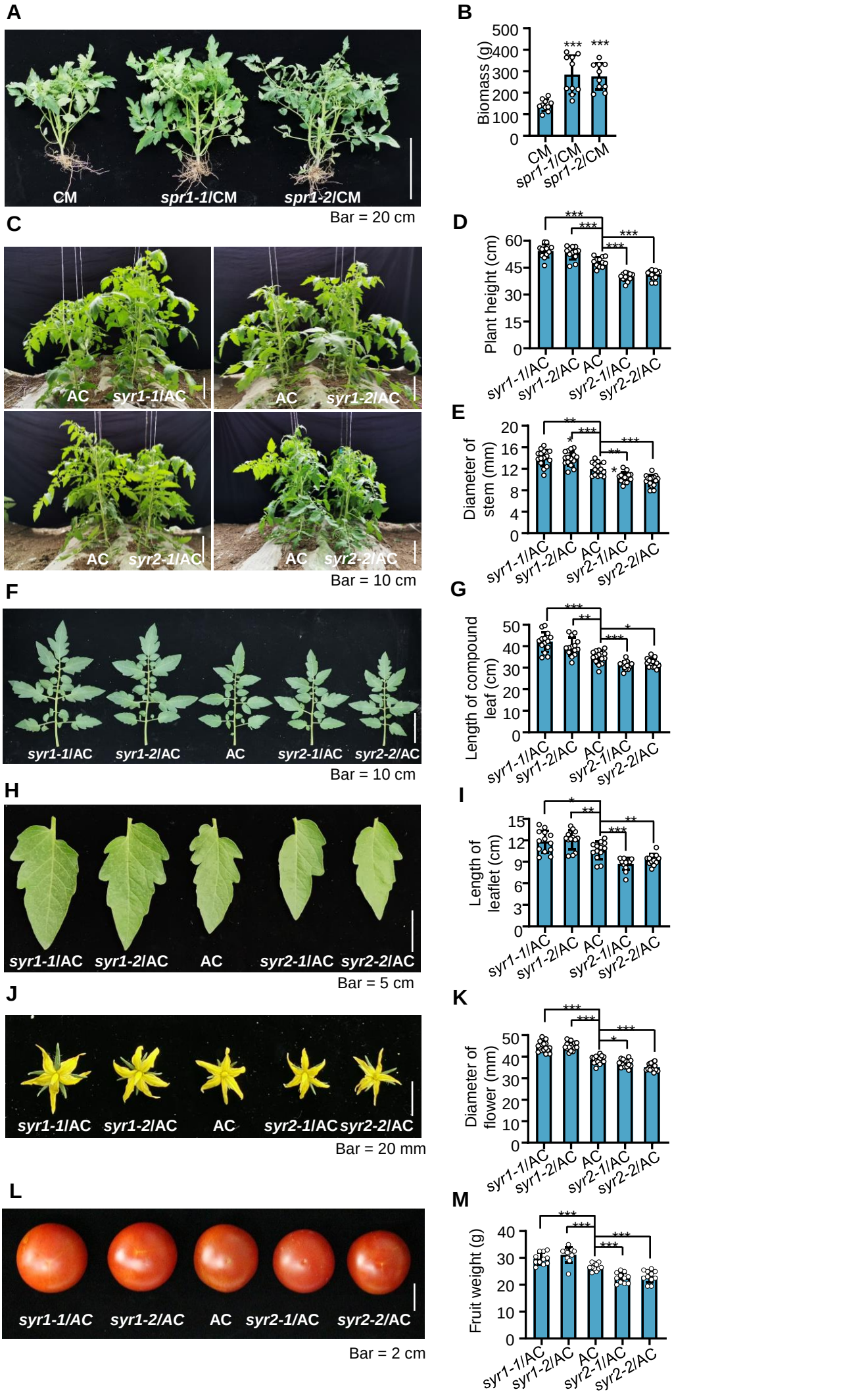
A
CM
spr1-1/CM
spr1-2/CM
Bar = 20 cm
B
Biomass (g)
500
400
300
200
100
0
***
***
CM
spr1-1/CM
spr1-2/CM
C
AC
syr1-1/AC
AC
syr1-2/AC
AC
syr2-1/AC
AC
syr2-2/AC
Bar = 10 cm
D
Plant height (cm)
60
45
30
15
0
***
***
***
***
syr1-1/AC
syr1-2/AC
AC
syr2-1/AC
syr2-2/AC
E
Diameter of stem (mm)
20
16
12
8
4
0
**
*
***
**
*
***
syr1-1/AC
syr1-2/AC
AC
syr2-1/AC
syr2-2/AC
F
syr1-1/AC
syr1-2/AC
AC
syr2-1/AC
syr2-2/AC
Bar = 10 cm
G
Length of compound leaf (cm)
50
40
30
20
10
0
***
**
*
***
syr1-1/AC
syr1-2/AC
AC
syr2-1/AC
syr2-2/AC
H
syr1-1/AC
syr1-2/AC
AC
syr2-1/AC
syr2-2/AC
Bar = 5 cm
I
Length of leaflet (cm)
15
12
9
6
3
0
*
**
***
**
syr1-1/AC
syr1-2/AC
AC
syr2-1/AC
syr2-2/AC
J
syr1-1/AC
syr1-2/AC
AC
syr2-1/AC
syr2-2/AC
Bar = 20 mm
K
Diameter of flower (mm)
50
40
30
20
10
0
***
***
*
***
syr1-1/AC
syr1-2/AC
AC
syr2-1/AC
syr2-2/AC
L
syr1-1/AC
syr1-2/AC
AC
syr2-1/AC
syr2-2/AC
Bar = 2 cm
M
Fruit weight (g)
40
30
20
10
0
***
***
***
***
syr1-1/AC
syr1-2/AC
AC
syr2-1/AC
syr2-2/AC

Figure S5. *SYR* mutations have distinct effects on plant growth and organ size, related to Figure 7

(A and B) Representative image (A) and biomass (B) of 48-d-old plants of indicated genotypes. Data are mean ± SD, *n* = 10 plants. Tomato cv. Castlemart (CM) was the WT of *spr1* mutants.

(C) Representative image of 58-d-old plants of the indicated genotypes. Scale bar, 10 cm.

(D) Height of 58-d-old plants of indicated genotypes. Data are mean ± SD, *n* = 12.

(E) Main stem diameter of 58-d-old plants of indicated genotypes. Data are mean ± SD, *n* = 15.

(F) Representative compound leaf of 58-d-old plants of indicated genotypes. Scale bar, 10 cm.

(G) Compound leaf length of 58-d-old plants of indicated genotypes. Data are mean ± SD, *n* = 14.

(H) Representative leaflet of 58-d-old plants of indicated genotypes. Scale bar, 5 cm.

(I) Leaflet length of 58-d-old plants of indicated genotypes. Data are mean ± SD, *n* = 13.

(J) Representative flower of 80-d-old plants of indicated genotypes. Scale bar, 20 mm.

(K) Flower diameter of 80-d-old plants of indicated genotypes. Data are mean ± SD, *n* = 15.

(L) Representative fruit of plants of indicated genotypes at the red ripe stage. Scale bar, 2 cm.

(M) Fruit weight of plants of indicated genotypes at the red ripe stage. Data are mean ± SD, n = 10.

In (C) to (M): tomato cv. Ailsa Craig (AC) was the WT of *syr* mutants. In (B), (D), (E), (G), (I), (K), and (M): the error bars represent SD. *p <0.05, **p <0.01, ***p <0.001 (Student's *t* test).